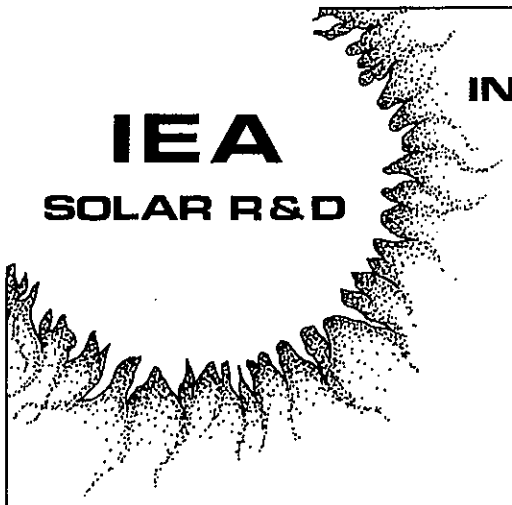

IEA

SOLAR R&D

INTERNATIONAL ENERGY AGENCY

program
to develop and test
solar heating
and cooling systems

task III
performance testing
of solar collectors

survey of solar simulator test facilities and initial results of IEA round robin tests using solar simulators

Deutsche Forschungs- und Versuchsanstalt
für Luft- und Raumfahrt e.V.,
Cologne, Fed. Republic of Germany, December 1979

INTERNATIONAL ENERGY AGENCY
PROGRAM TO DEVELOP AND TEST
SOLAR HEATING AND COOLING SYSTEMS

TASK III
PERFORMANCE TESTING OF SOLAR COLLECTORS

SUBTASK C

SURVEY OF SOLAR SIMULATOR TEST FACILITIES AND INITIAL RESULTS OF IEA ROUND ROBIN TESTS USING SOLAR SIMULATORS

W. LEY - DFVLR

Date: December 1979

DEUTSCHE FORSCHUNGS- UND VERSUCHSANSTALT FÜR
LUFT- UND RAUMFAHRT e.V., COLOGNE, FEDERAL REPUBLIC OF GERMANY
December 1979

This report is part of the work of the IEA Solar Heating and Cooling Program
Task III: Performance Testing of Solar Collectors
Subtask C: Survey of Solar Simulator Test Facilities and Initial Results of IEA Round Robin Tests Using Solar Simulators

Distribution: Unrestricted
Additional Copies can be ordered from:

Wilfried Ley
DFVLR
Postfach 906058
D-5000 Köln 90, Germany

Price: 12,-- DM

Deutsche Forschungs- und
Versuchsanstalt für Luft- und Raumfahrt e.V.
Cologne,
Federal Republic of Germany

PREFACE

INTERNATIONAL ENERGY AGENCY

In order to strengthen cooperation in the vital area of energy policy, an Agreement on an International Energy Program was formulated among a number of industrialized countries in November 1974. The International Energy Agency (IEA) was established as an autonomous body within the Organization for Economic Cooperation and Development (OECD) to administer that agreement. Nineteen countries are currently members of the IEA, with the Commission of the European Communities participating under a special arrangement.

As one element of the International Energy Program, the participants undertake cooperative activities in energy research, development, and demonstration. A number of new and improved energy technologies which have the potential of making significant contributions to our energy needs were identified for collaborative efforts. The IEA Committee on Energy Research and Development (CRD), assisted by a small Secretariat, coordinates the energy research, development, and demonstration program.

SOLAR HEATING AND COOLING PROGRAM

Solar Heating and Cooling was one of the technologies selected by the IEA for a collaborative effort. The objective was to undertake cooperative research, development, demonstrations and exchanges of information in order to advance the activities of all Participants in the field of solar heating and cooling systems. Several sub-projects or "tasks" were developed in key areas for solar heating and cooling. A formal Implementing Agreement for this Program, covering the contributions, obligations and rights of the Participants, as well as the scope of each task, was prepared and signed by 15 countries and the Commission of the European Communities. The overall program is managed by an Executive Committee, while the management of the sub-projects is the responsibility of the Operating Agents who act on behalf of the other Participants.

The tasks of the IEA Solar Heating and Cooling Program and their respective Operating agents are:

I. Investigation of the Performance of Solar Heating and Cooling Systems -
Technical University of Denmark

II. Coordination of R & D on Solar Heating and Cooling Components -
Agency of Industrial Science and Technology, Japan

III. Performance Testing of Solar Collectors -
Kernforschungsanlage Jülich, Federal Republic of Germany

IV. Development of an Insolation Handbook and Instrumentation Package -
United States Department of Energy

V. Use of Existing Meteorological Information for Solar Energy Application -
Swedish Meteorological and Hydrological Institute.

Collaboration in additional areas is likely to be considered as projects are completed or fruitful topics for cooperation identified.

TASK III - PERFORMANCE TESTING OF SOLAR COLLECTORS

A wide variety of collector designs with a broad range of qualitative differences exists. Since the collector is the key component in an active solar system, performance testing is a vital task. The objective of Task III is to develop internationally accepted test procedures for rating the thermal performance as well as the reliability and durability of collectors. This project is also experimenting with the use of solar simulators to allow year-round testing of collectors.

The subtasks of this project are:

A. Development and Application of Standard Test Procedures for Determining Thermal Performance
B. Development of Reliability and Durability Test Procedures
C. Investigation of the Potential of Solar Simulators

The following countries are participants in Task III: Austria, Belgium, Canada, Denmark, Germany, Greece, Italy, Japan, the Netherlands, New Zealand, Spain, Sweden, Switzerland, United Kingdom, USA, and the Commission of the European Communities.

This report documents work carried out under subtask C of this Task. The cooperative work and resulting report is described in the following section.

SUMMARY

The International Energy Agency (IEA) in cooperation with a number of participating countries investigates and evaluates standard solar collector test methods for the determination of the thermal performance of flat-plate solar collectors on an international basis. The thermal efficiency of two water heating flat-plate solar collectors (Chamberlain and Commercial Solar Energy) was obtained indoors using solar simulators.

Solar simulators show good promise to potentially provide test results that are both reproducible and correlate well to outdoor performance. The use of a solar simulator is particularly attractive for testing a collector because each parameter may be varied independently to determine the full range of performance characteristics.

However, future work has to be focussed on the identification of the performance features of solar simulators, because the differences found in the initial results of IEA round robin tests seem to be strongly associated with the functional characteristics of the solar cimulators which were not sufficiently evaluated at this interim phase of the program.

LIST OF PARTICIPANTS IN THE SOLAR SIMULATOR ROUND ROBIN TESTS

Key to Participants	Collector No. 1	Collector No. 2
1. Solar Research Lab. The Government Industrial Research Institute Nagoya Nagoya/Japan S. Tanemura	x	x
2. Solar Energy Unit University College Cardiff/United Kingdom W. B. Gillett	x	x
3. Statens Provningsanstalt Boras/Sweden H. E. B. Andersson	x	x
4. Deutsche Forschungs- und Versuchsanstalt für Luft- und Raumfahrt, DFVLR Köln-Porz/Germany W. Ley	x	x
5. Technical University of Denmark Thermal Insulation Lab. Lyngby/Denmark S. Svendsen	x	
6. National Bureau of Standards Washington/USA E. Streed	x	
Honeywell Research Facility Minneapolis/Minnesota J.D. Kopecky		
7. National Bureau of Standards Washington/USA E. Streed	x	x
Boeing Aerospace Co. Seattle/Washington A. R. Lundy		

TABLE OF CONTENTS

1. INTRODUCTION

The promotion of solar technology in recent years has made evident the need for standardized procedures allowing for rating solar collectors. The efforts at most places have focussed on the development of a procedure to determine the efficiency of the collector over a range of operating temperatures. While it is well understood that collector array performance is dependent upon system type and operation, it is considered necessary to provide thermal performance data for individual collector panels for comparison of collectors and for system design. The methods of testing collectors should be generally applicable, practical and provide guidance for precise and accurate measurements. The evaluation of the procedure became the object of the program.

A round robin test program in the U.S. [3] was already under way when the IEA-program was defined. Moreover, the IEA round robin test - being international in scope - provided the unique chance of an evaluation of standard procedures by many countries based on common experience. The program initiated was not confined to a particular procedure but the NBS-method published in 1974 [1] (used as the basis for ASHRAE-Standard 93-77 [4]) formed a basis to start with. A second procedure, the BSE-method [2], came into being in the course of the program. These procedures subjected to amendments and supplemented by additional tests were applied to two collectors, in both outdoor and indoor test facilities. Due to varying climatic conditions outdoor tests of solar collectors can, however, be very timeconsuming. Use of solar simulators for testing is attractive to the European nations due to the lack of clear test days in northern European climates and on the assumption that simulators will provide more reproducible results than outdoor tests.

Thermal performance measurements were conducted by some Participants with an indoor solar collector test facility using a solar simulator. Reproducible measurements with a solar simulator under standard test conditions for solar irradiance, solar spectral distribution, flow rate, fluid inlet temperature, ambient temperature and wind speed allow a comparison of the performance between the two solar collector types.

During the course of the IEA program new solar simulators have been designed and comissioned. Most of the new simulators are considered by their laboratories to be in a stage of development, and the results reported must therefore be studied with caution. It must be expected that further developments will take place in the field of solar simulator testing in the near future, and these developments are likely to result in modifications to existing facilities, test procedures and instrumentation. New solar simulators are also known to be under construction.

A comparative evaluation of the outdoor and indoor (with a solar simulator) thermal performance measurements was conducted.

2. DESCRIPTION OF FACILITIES

A summary of solar simulator characteristics is given in table 1 showing the status of the solar simulators which have been used in this program.

In the following a short description of installed solar simulators is given.

1. Solar Research Laboratory
   Government Industrial Research Institute Nagoya
   Nagoya/Japan
   S. Tanemura

The Solar Research Laboratory has no solar simulator available. The solar simulator used for the IEA Round Robin Tests is installed at the Oyama plant of Showa Aluminium Co. Ltd. which is located 300 km away from their laboratory.
The test installation set up in Showa Aluminium Co., Oyama plant, Japan, was used for the indoor testing. The installation schematic is shown in Figures 1 and 2. The solar simulator is similar to one formerly at the NASA Lewis Center. The radiation source consists of 187 tungsten-halogen lamps (GE-2/H-300W) with dichroic coated reflectors. Each lamp has a graded acrylic resin fresnel lens (Cryton Optics Co.) to collimate its output.
The lamps and lenses are air-cooled by circulation of air in the lamp system as shown in Figure 3. The distance from the lamp system to the test plane is 4.6 m. The dimensions of the test plane are 1.2 m (W) x 1.8 m (L). The uniformity of the irradiance of the solar simulator is less than ± 5 % in the test plane. The collimation is such that 95 % of the energy output is within a subtended angle of less than 9° in arc. The air mass 2 spectral distribution is obtained on the test plane with a lamp voltage of about 105 V-AC for an irradiance of 757 W/m^2 as shown in Figure 4. The inlet fluid temperature is controlled at a specified value within an accuracy of ± 0.4° C during the testing period by electric heater, magnetic valve and heat exchanger.

A six junction Cu-Constantan thermopile is used for the fluid temperature measurement. The length of the pipe between the device and collector inlet/outlet is about 20 cm. Both the device and the pipe are insulated by glass wool.

The wind load on the collector surface, simulated by two air blowers can be adjusted in the range from 0 to 5 m/sec.
For further technical details see Tables 1 and 2.

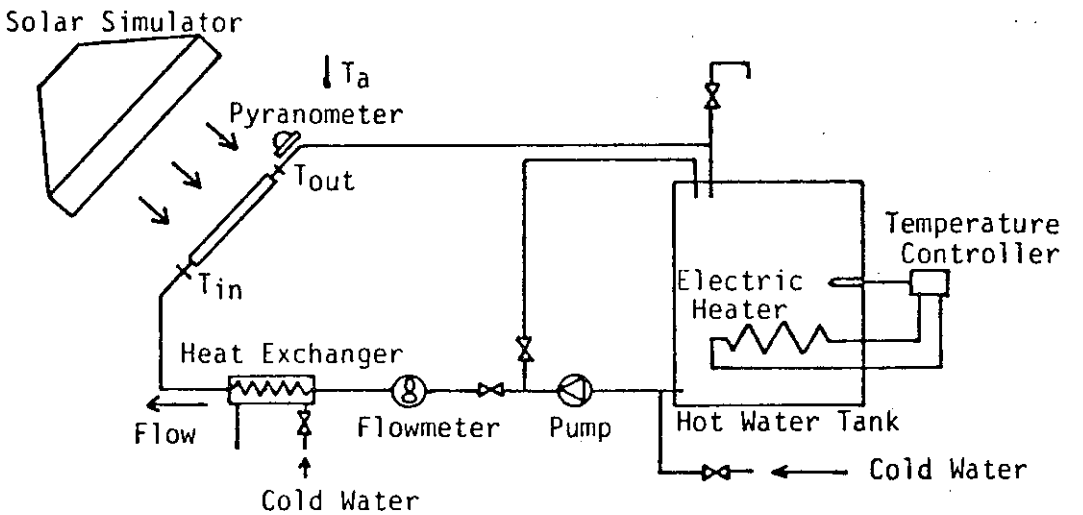

Figure 1 Scheme of Test Installation

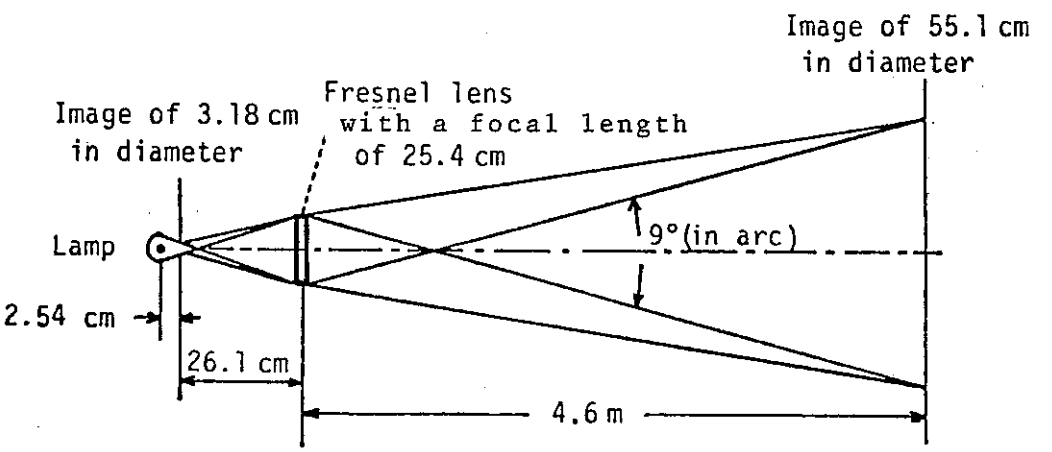

Figure 2
Schematic View of the Collimation System of each Lamp. Collector Test Plane is located 4.6 m from the Lens Surface.

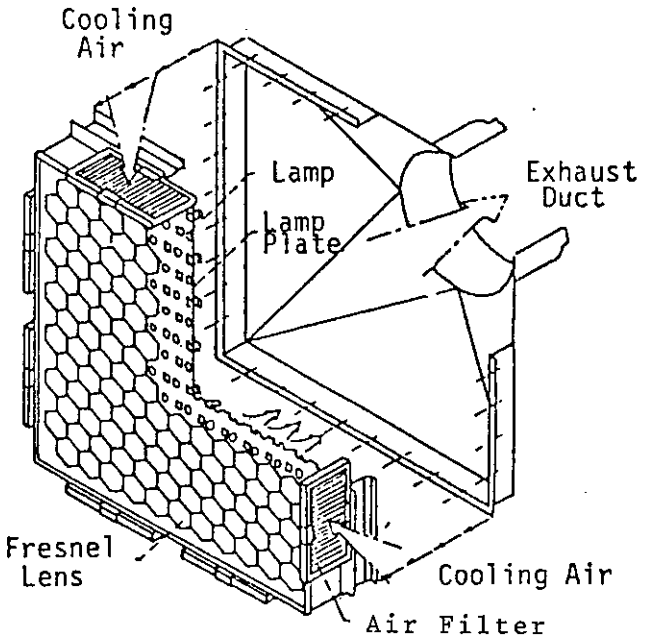

The lenses are cooled by forced convection with air

Figure 3 Schematic View of the Light Source of the Solar Simulator

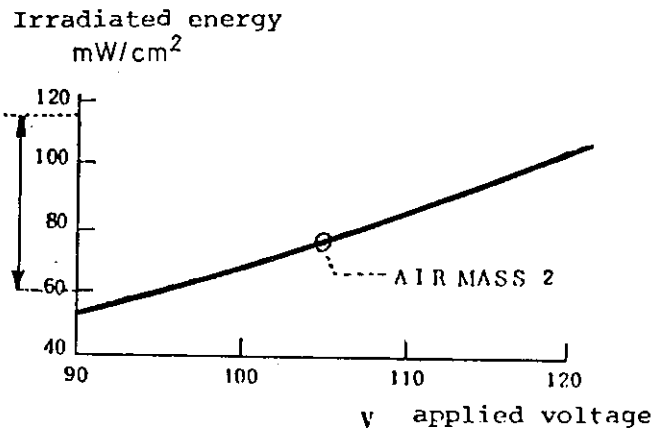

Figure 4 Irradiated Energy versus applied Lamp Voltage. Air Mass 2 Spectrum can be obtained at 105 V-AC.

2 Solar Energy Unit
University College
Cardiff/United Kingdom
W.B. Gillett

The SRC solar simulator at Cardiff, which was the first to use the Thorn Compact Source Iodide lamp, was designed in 1975. It has 19 C.S.I. lamps (1 kW each) which produce a close match to the A.M.2 solar spectrum. The maximum irradiance is 900 W/m^2, for a test area of 2.25 m in diameter. The wind velocity across the collector can be varied from 0 to 10 m/s. The simulator has not only a variable collector tilt angle, but also the altitude of the lamp array can be varied through a full 90 degrees of arc. (see Figures 5 and 6).
For further technical details of the solar simulator see Tables 1 and 2.

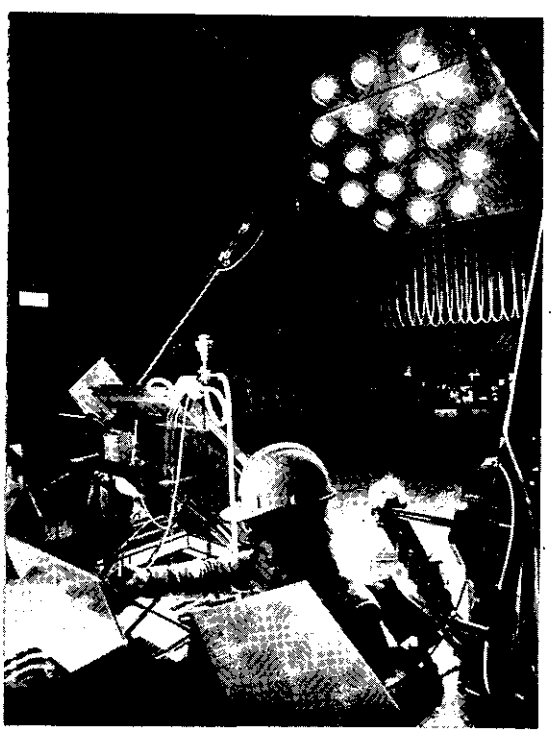

Figure 5 **SRC Solar Simulator**

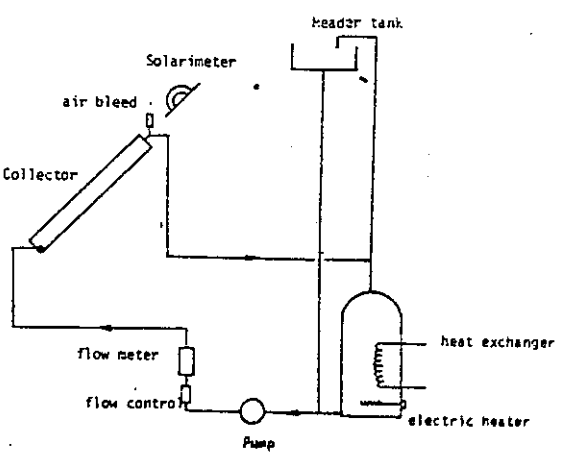

Fig. 6.1 Diagram of Collector test loop

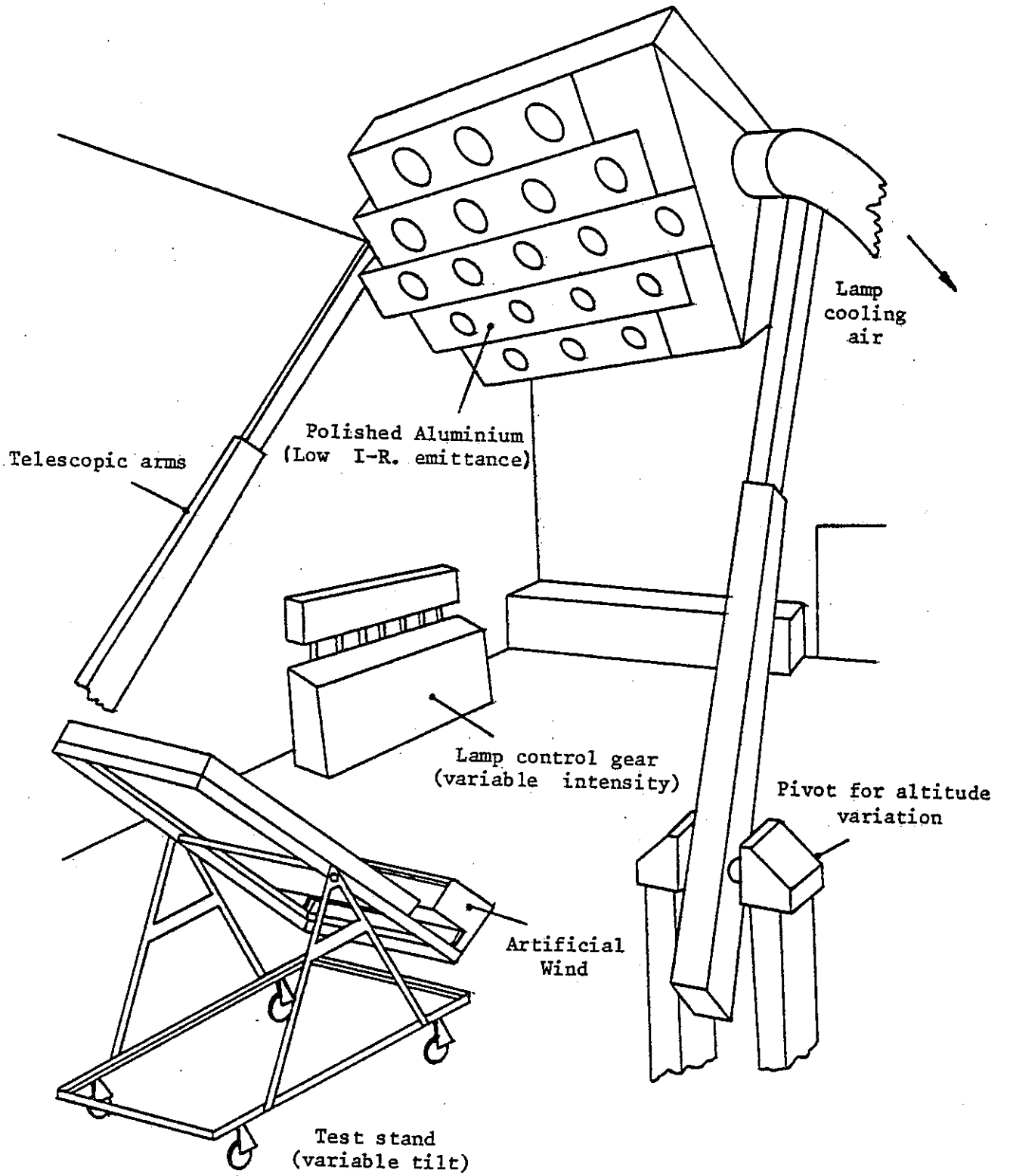

Figure 6.2 SRC solar simulator

3 Statens Provningsanstalt
Boras/Sweden
H. E. B. Andersson

The aim was to build a cheap simulator which was easy to handle for routine tests of collectors. Therefore a commercially available lamp was looked for which would include the necessary optics and have a spectrum which could be used without filtering. Besides, effort has been put into the development of an efficient data acquisition system, so that collected data can be transferred automatically to a test report.

A 1 kW sealed beam compact source mercury iodide lamp is used. The lamp, CSI 1000, is made by Thorn Lighting Ltd., London. Measured data for the lamp are given below.

The spectral distribution was measured for several directions, positions and levels of mains power. Comparisons were made between the solar spectrum airmass 2 and the lamp spectrum. The diagram curves were normalized to equal integrated values.

Fig. 7a shows the relative spectral radiant intensity measured on the symmetry line of the lamp when the beam is horizontal. Measurement values were taken with 25 nm half value bandwidth, which is much larger than that of the spectral lines. The real peak values of these lines are much higher than shown in the diagram. Nevertheless the overall distribution of the spectral irradiation is rather close to the requirements given by ASHRAE.

Spectral distribution

λ (nm)	CSI-1000(%)	ASHRAE(%)
300 - 400	1,7	2 - 3
400 - 700	49	35 - 53
700 -1000	21	26 - 32
1000 -2500	28	14 - 34

Fig 7 shows the simulator. The lamp frame can be tilted and moved up and down. It can be moved along the room, which has dimensions 12 x 8 m^2 and 6 m in height.

Fig. 7b shows a block diagram of the system. The central unit in the system is an HP 9825 desk computer. It is equipped with a scanner and a home made control unit containing power regulator for the lamps and measuring instruments for the pyranometers, the thermometers and the flow meter.

Nine pyranometers, Lambda LI-200S, mounted on a ramp, are used to measure the irradiance. The detector ramp is moved stepwise by a step motor across the test surface. Each detector is connected to a voltage/frequency converter.

The calibration is performed using the solar simulator and an Eppley PSP pyranometer.

For further technical details see Tables 1 and 2.

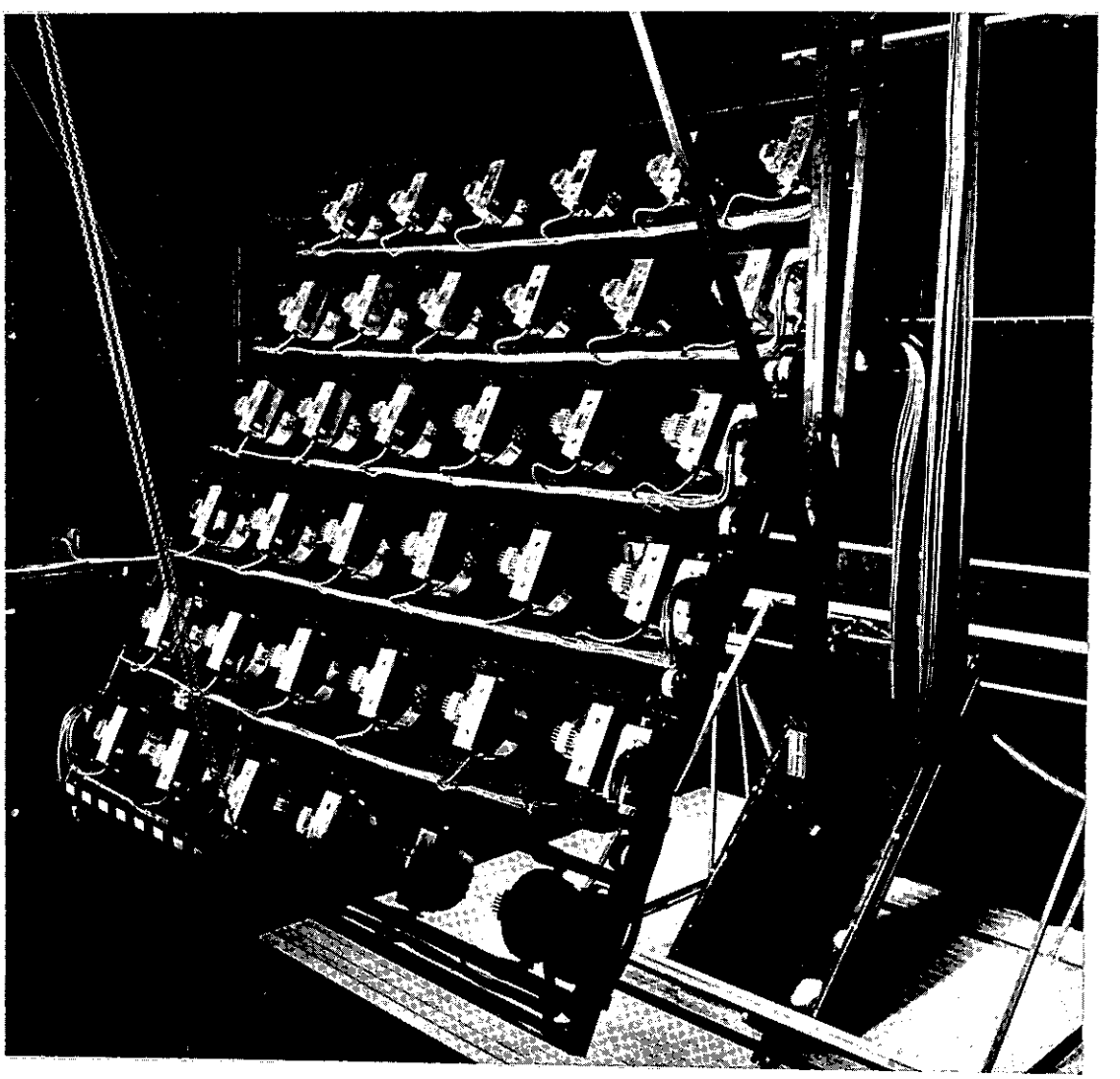

Figure 7 The solar simulator test stand.

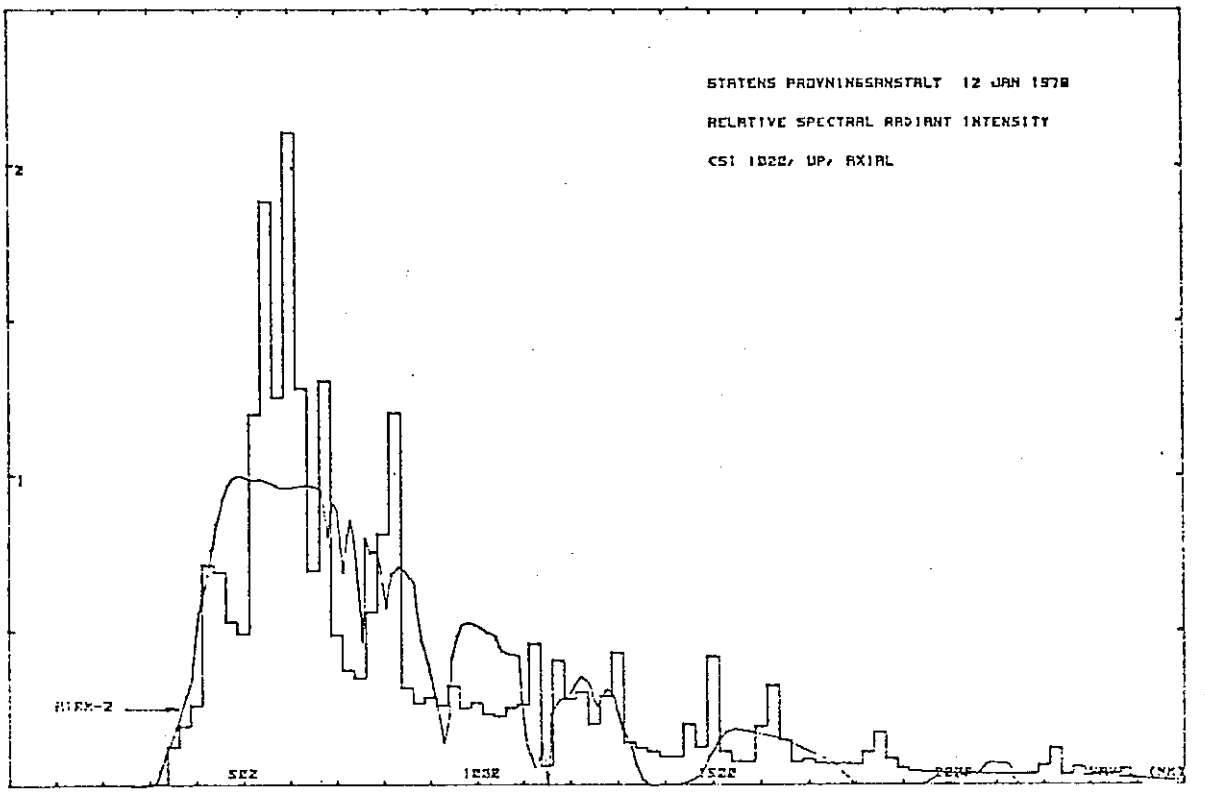

Figure 7a Relative spectral radiant intensity for the CSI 1000 lamp.

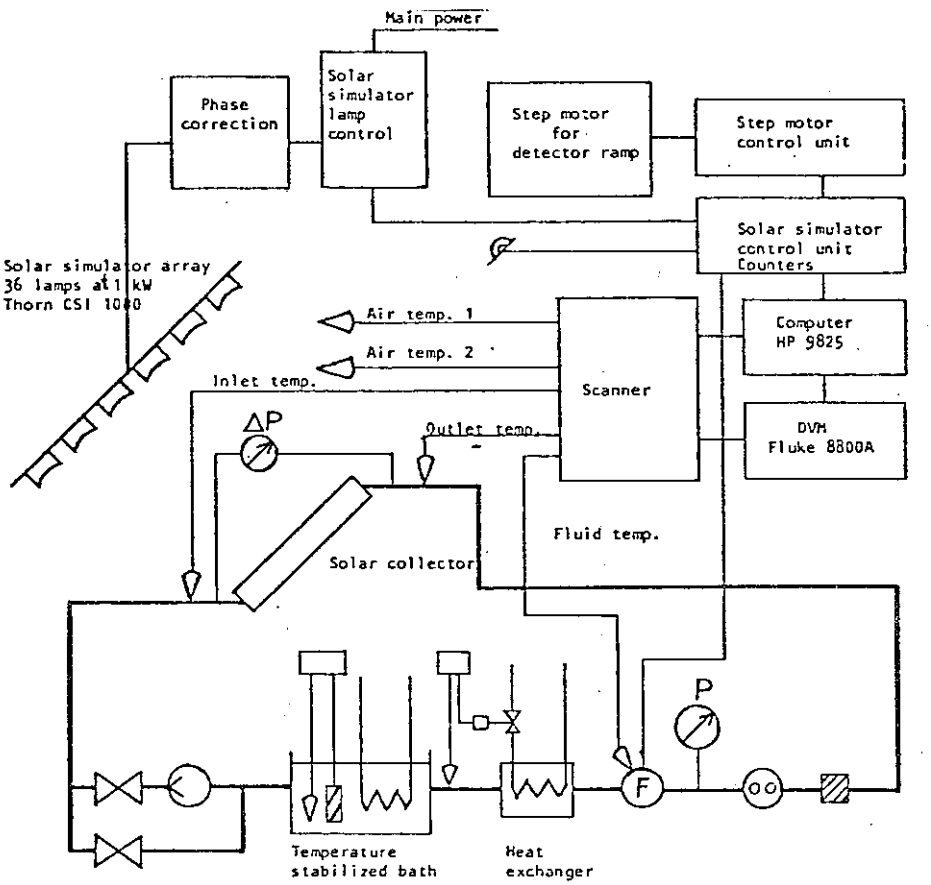

Figure 7b Diagram of the solar simulator system and test stand.

4 Deutsche Forschungs- und Versuchsanstalt
für Luft- und Raumfahrt, DFVLR
Köln-Porz/Germany
W. Ley

Technical data of the DFVLR solar simulator

Optical system	: ON-AXIS, divergent radiation
Divergence half angle	: maximum 9^{o}
Radiation source	: 10 xenon lamps (6.5 kW each)
Life time of lamps	: 600 h
Spectral distribution	: adaptation to the AM0 spectrum or to the AM2 spectrum by the use of additional filters
Diameter of reference area	: 1.6 m
Irradiance	: 100-1700 W/m^2 1 SC = 1370 W/m^2
Irradiance uniformity	: $<\pm$ 5 %

The solar simulator can be operated up to 600 hours before the lamps have to be exchanged which requires a readjustment of the optical unit.

The automatic control of the irradiance is capable of maintaining the required irradiance during the total test period to ± 0.5 %.

The spectral distribution of the solar radiation can be varied from extraterrestrial (AM0-spectrum) to terrestrial AM2 spectrum by the use of additional filters. The spectral distribution in the test area is measured with a spectral photometer. The solar simulator and indoor test facility is shown in Figures 8,9,10,11, and 12.
For further technical details see Tables 1 and 2.

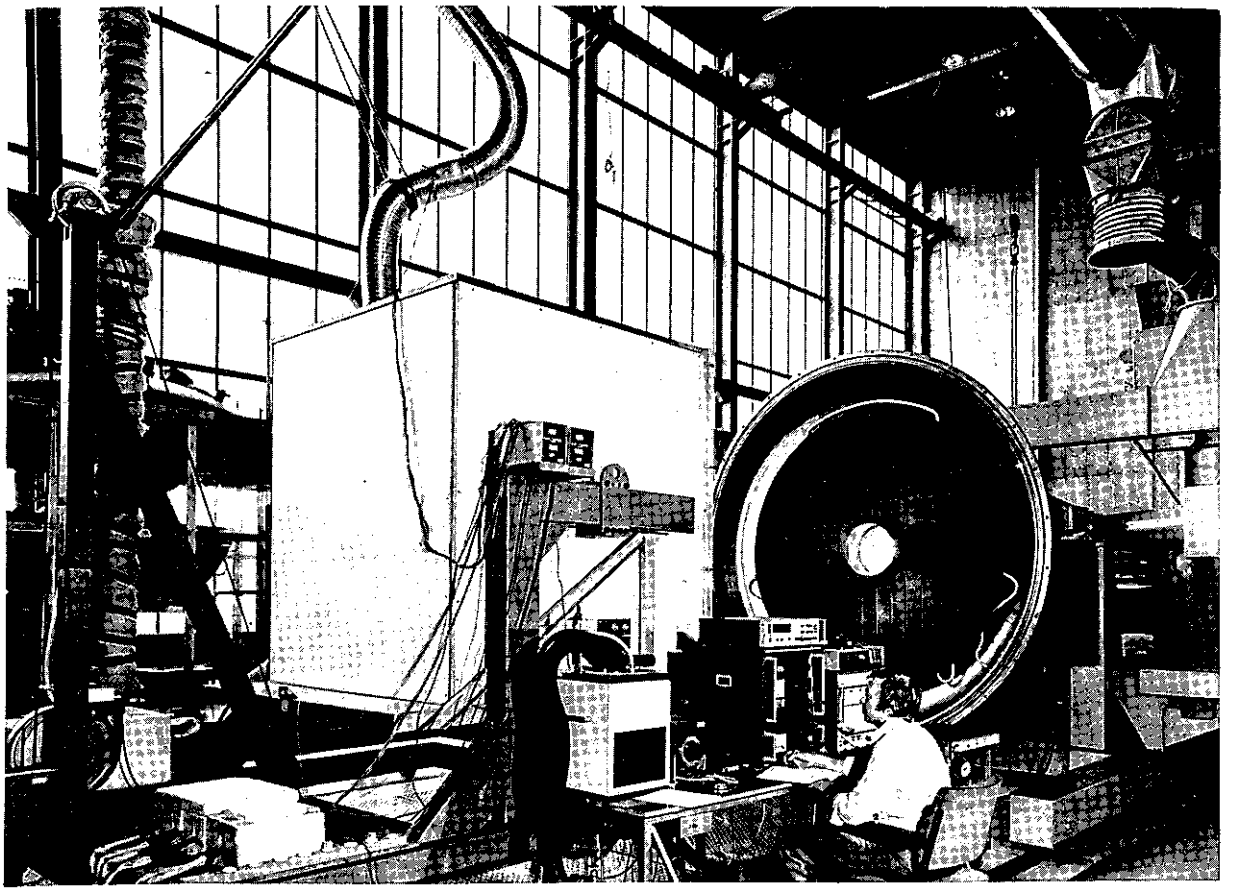

Figure 8 Indoor Solar Collector Test Facility of the DFVLR in Cologne

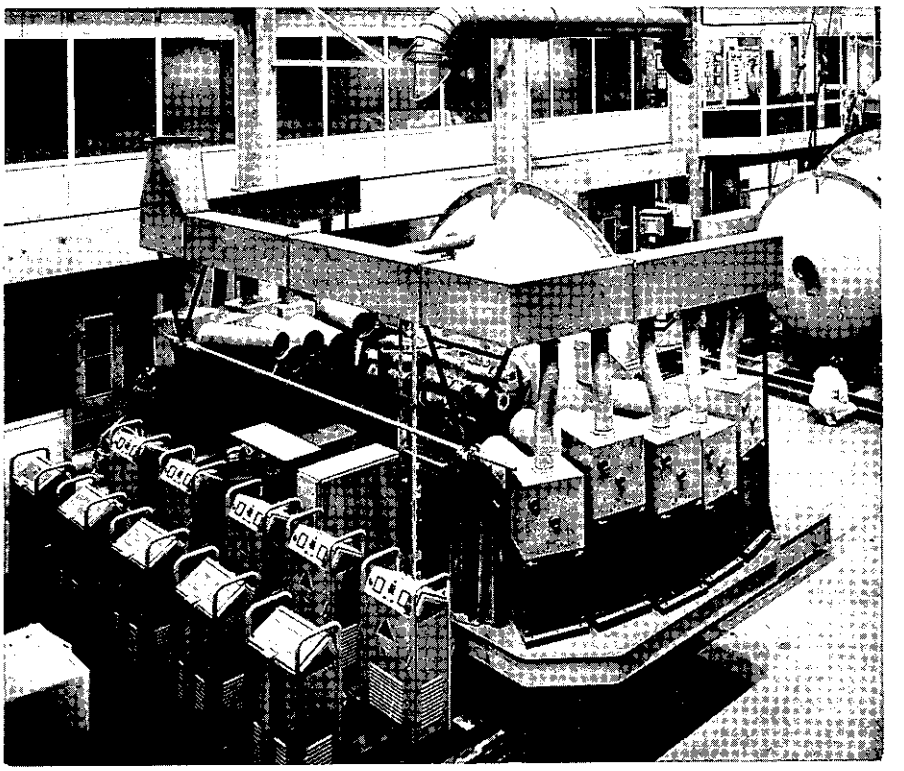

Figure 9 Solar Simulator

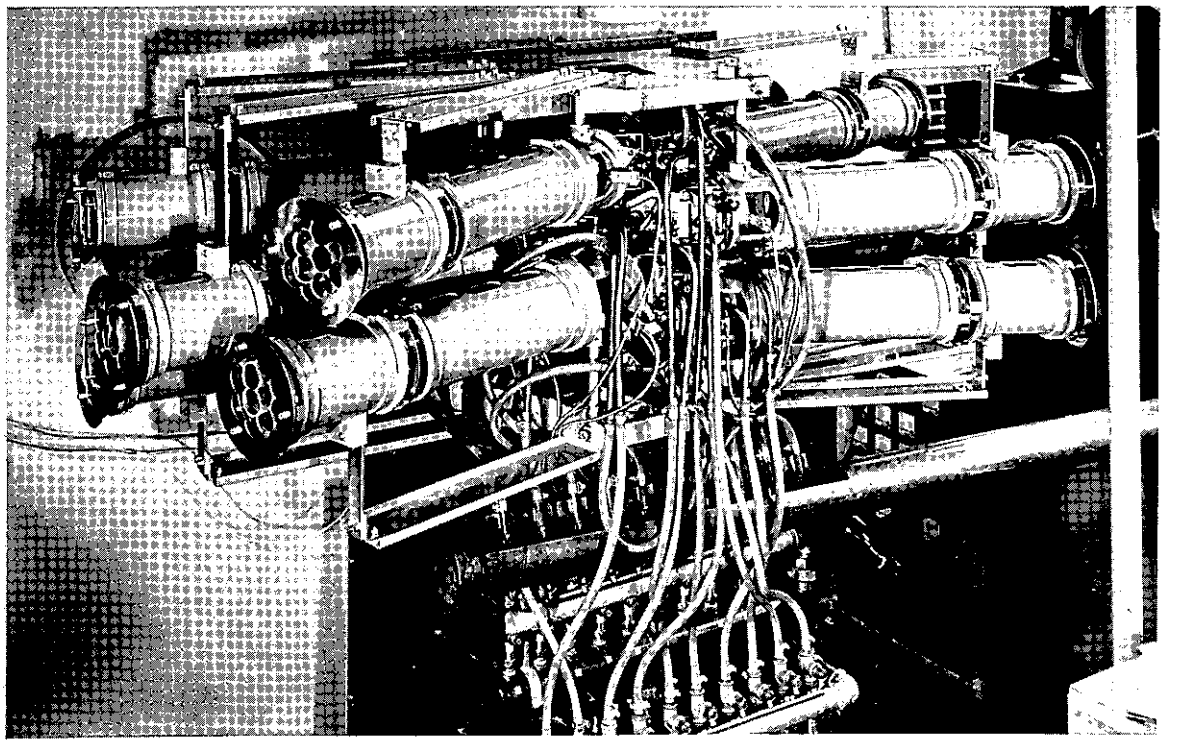

Figure 1o Integration Lens System of the Solar Simulator

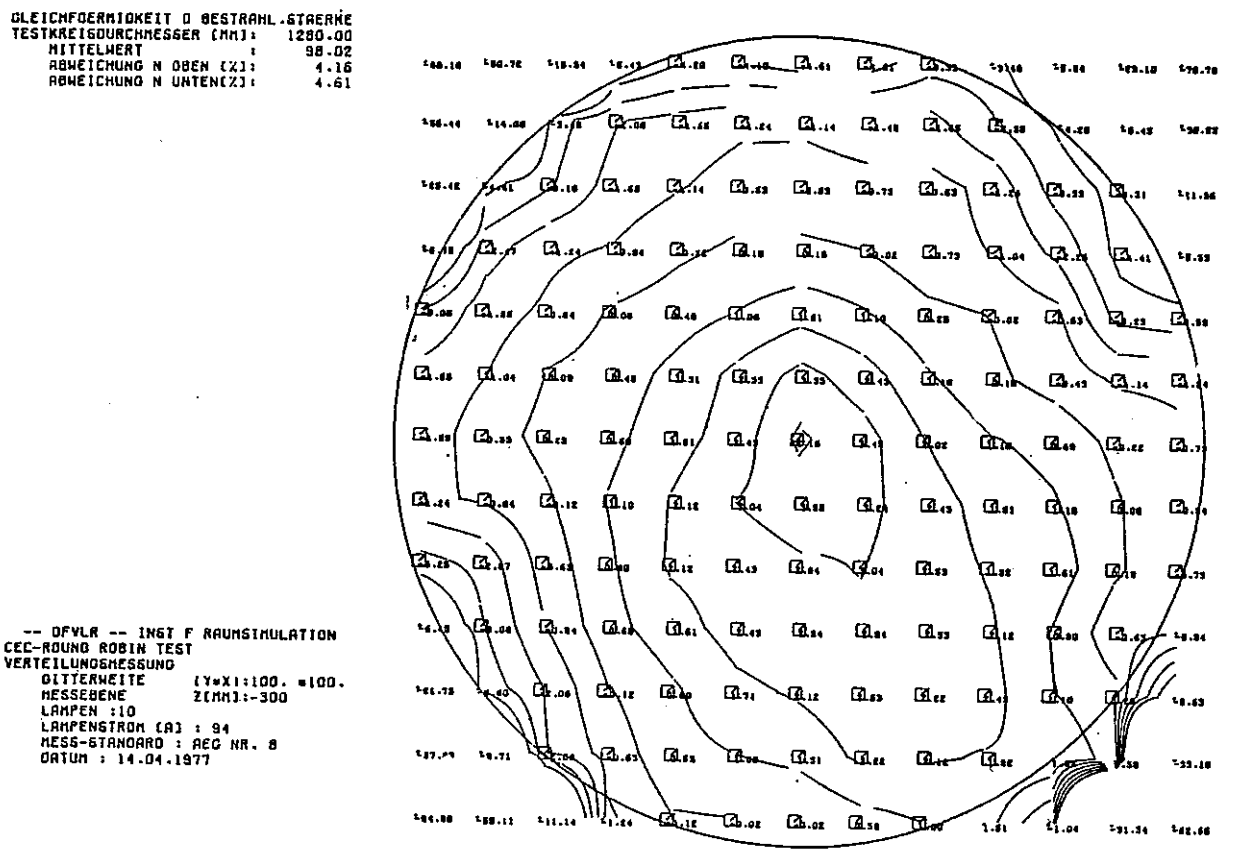

Figure 11 Uniformity Distribution

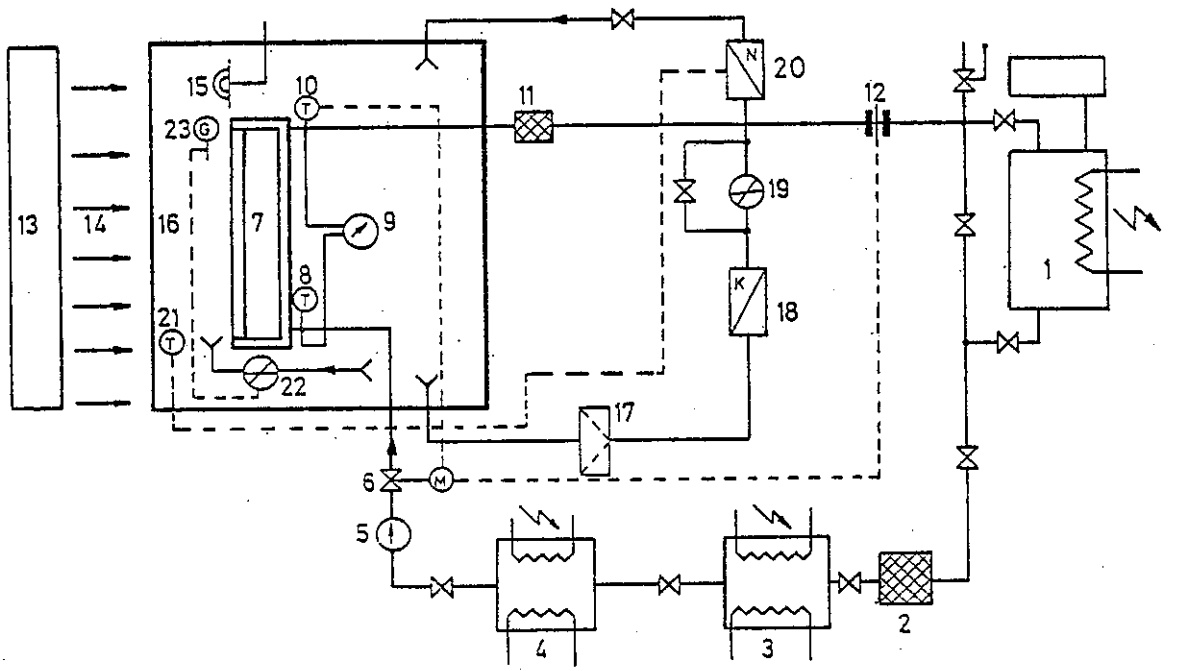

1. Thermal storage tank with heaters
2. Fine-mesh filter
3. Tempering bath - Coarse control
4. Tempering bath - Fine control
5. Fluid feed pump
6. Throttle of mass flow, controlled by constant outlet temperature or constant mass flow rate
7. Solar collector
8. Measuring point of fluid inlet temperature
9. Pressure difference of solar collector
10. Measuring point of fluid outlet temperature
11. Fine-mesh filter
12. Flow measurement
13. Solar simulator
14. Artificial global radiation
15. Measuring point of intensity measurement
16. Test compartment for constant ambient conditions
17./18./19./20. Equipment for constant ambient temperature within the test compartment
21. Measuring point of ambient temperature within the test compartment
22. Equipment for simulation of wind velocity
23. Measurement point of wind velocity

Figure 12 Scheme of Coolant Flow Loop

5 Technical University of Denmark
Thermal Insulation Lab.
Lyngby/ Denmark
S. Svendsen

The solar simulator at the Technical University of Denmark has 36 compact source iodide lamps (1 kW each). The spectrum of the solar simulator is matched to the AM2 spectrum. The maximum irradiance is 1200 W/m^2 for a test area of 1.2 m x 2.4 m. The wind velocity across the collector can be varied from 0 to 10 m/s. The solar simulator is shown in Figures 13 and 14. For further technical details see Tables 1 and 2.

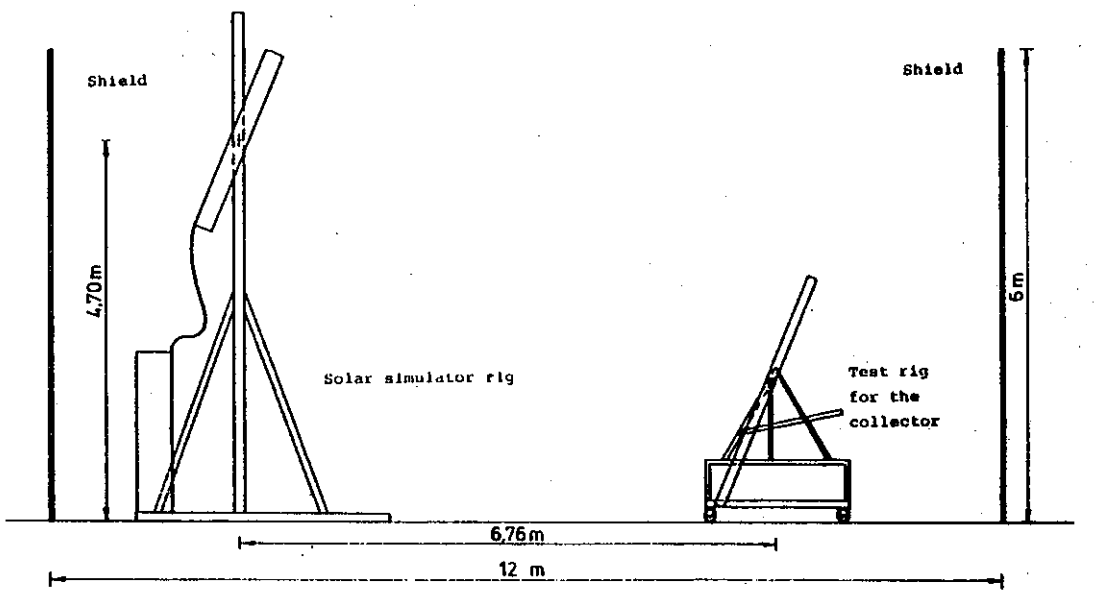

Figure 13 Solar Simulator Installation

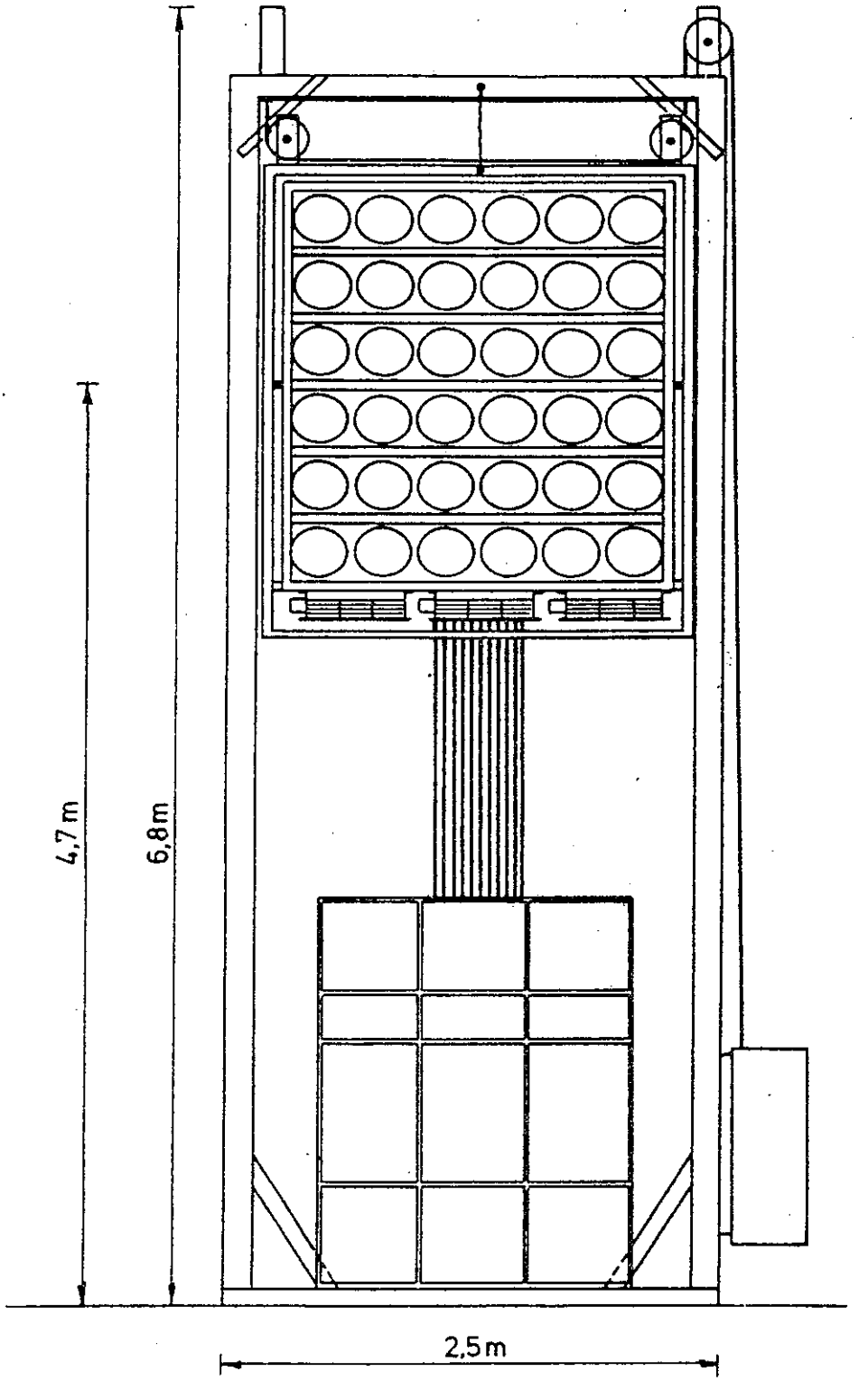

Figure 14 Solar Simulator

6 National Bureau of Standards
Washington/USA
E. Streed

Honeywell Research Facility
Minneapolis/Minnesota
J. D. Kopecky

The solar simulator at the Honeywell Research Facility incorporates 200 Tungsten-Halogen Lamps (300 W each). The spectrum of the solar simulator is matched to the AM2 spectrum. The maximum irradiance is 1460 W/m^2 for a test area of 1.6 m^2. This facility is identical to one built at NASA Lewis Research Center. A similar solar simulator equipped with 405 lamps to provide a test area of 3.1 m^2 is currently in operation at the NASA Marshall Space Flight Center, Huntsville, Alabama. The typical collector set up for the simulator facility is shown in Figures 15 and 16. For further technical details see Table 1.

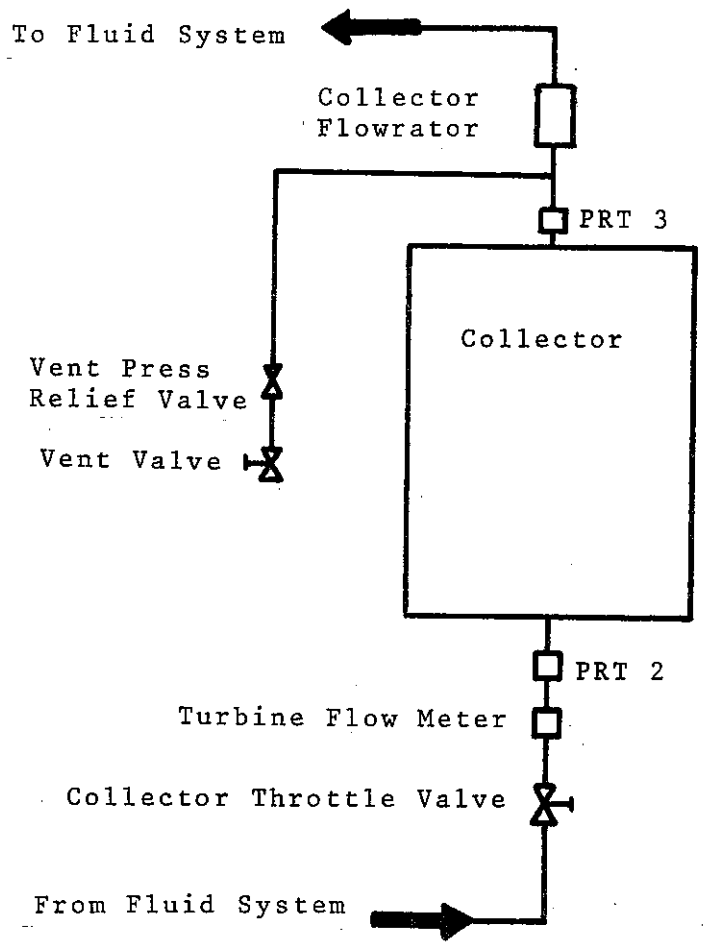

Figure 15 Collector Set Up for Simulator Facility

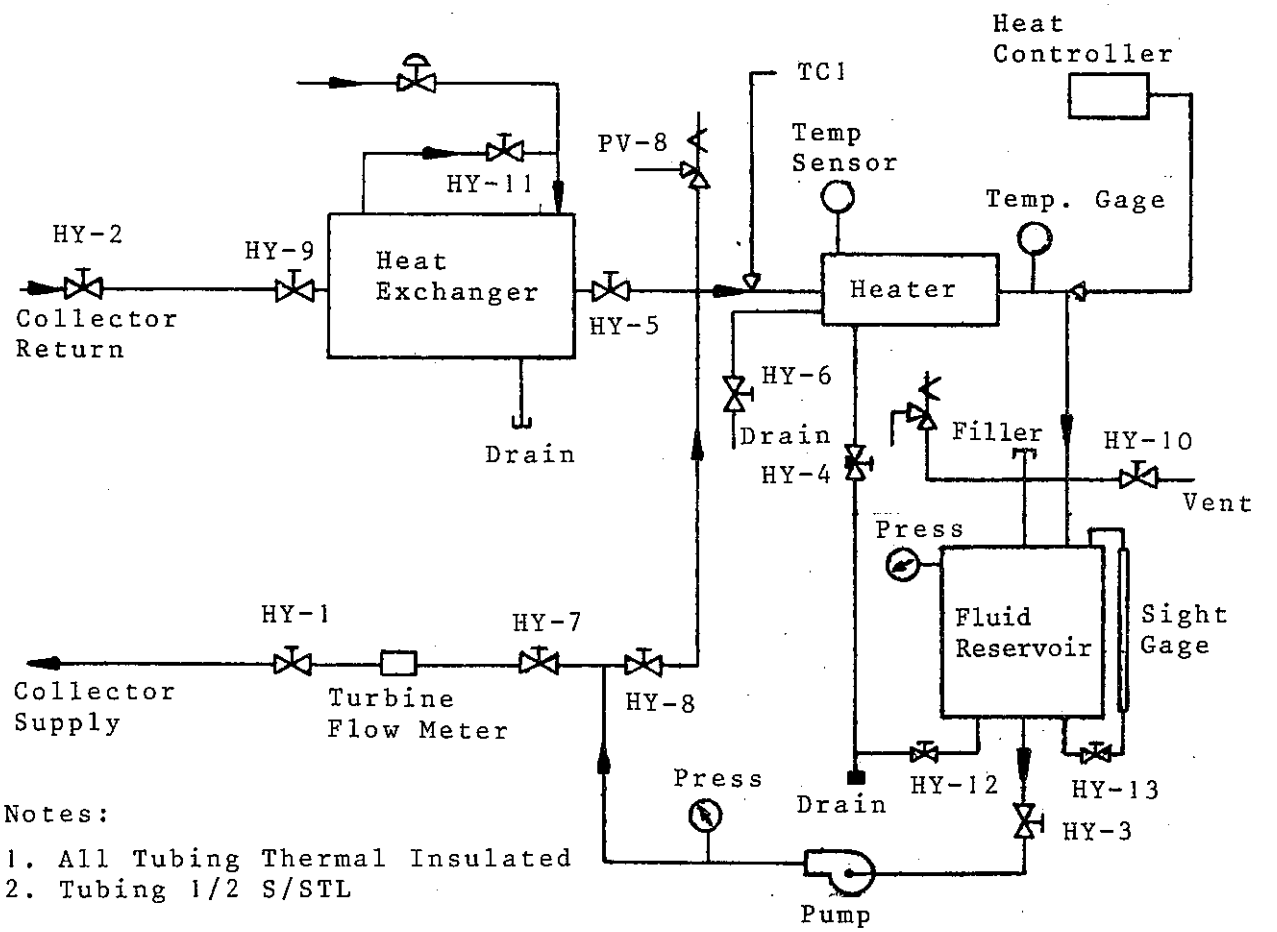

Figure 16 Collector Liquid Test Loop Flow Diagram

7 National Bureau of Standards
Washington/USA
E. R. Streed

Boeing Aerospace Co.
Seattle/Washington
A. R.Lundy

The solar simulator at Boeing Aerospace Co. has 7 Xenon short arc lamps (20 kW each). The spectrum of the solar simulator is matched to the AM0 spectrum and can be filtered to the AM2 spectrum. The maximum irradiance is 2950 W/m^2 for a test area of 7.0 m^2. The solar simulator and the collector test loop are shown in Figures 17 and 18. For further technical details see Tables 1 and 2.

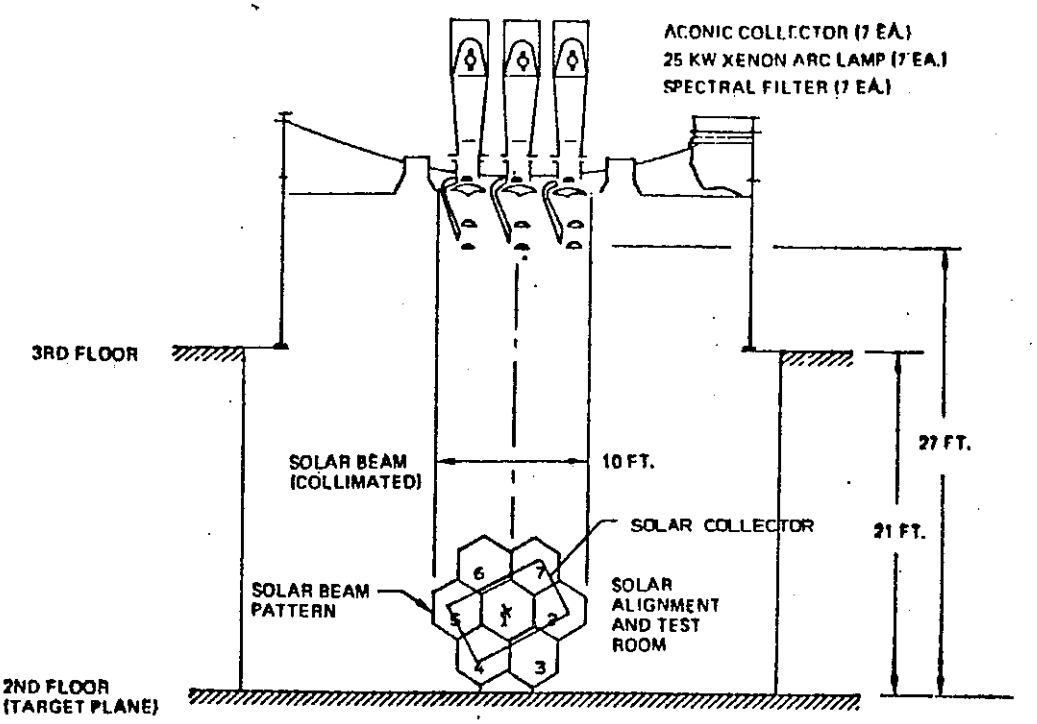

Figure 17 Boeing Aerospace Co. A-7ooo Solar Simulator

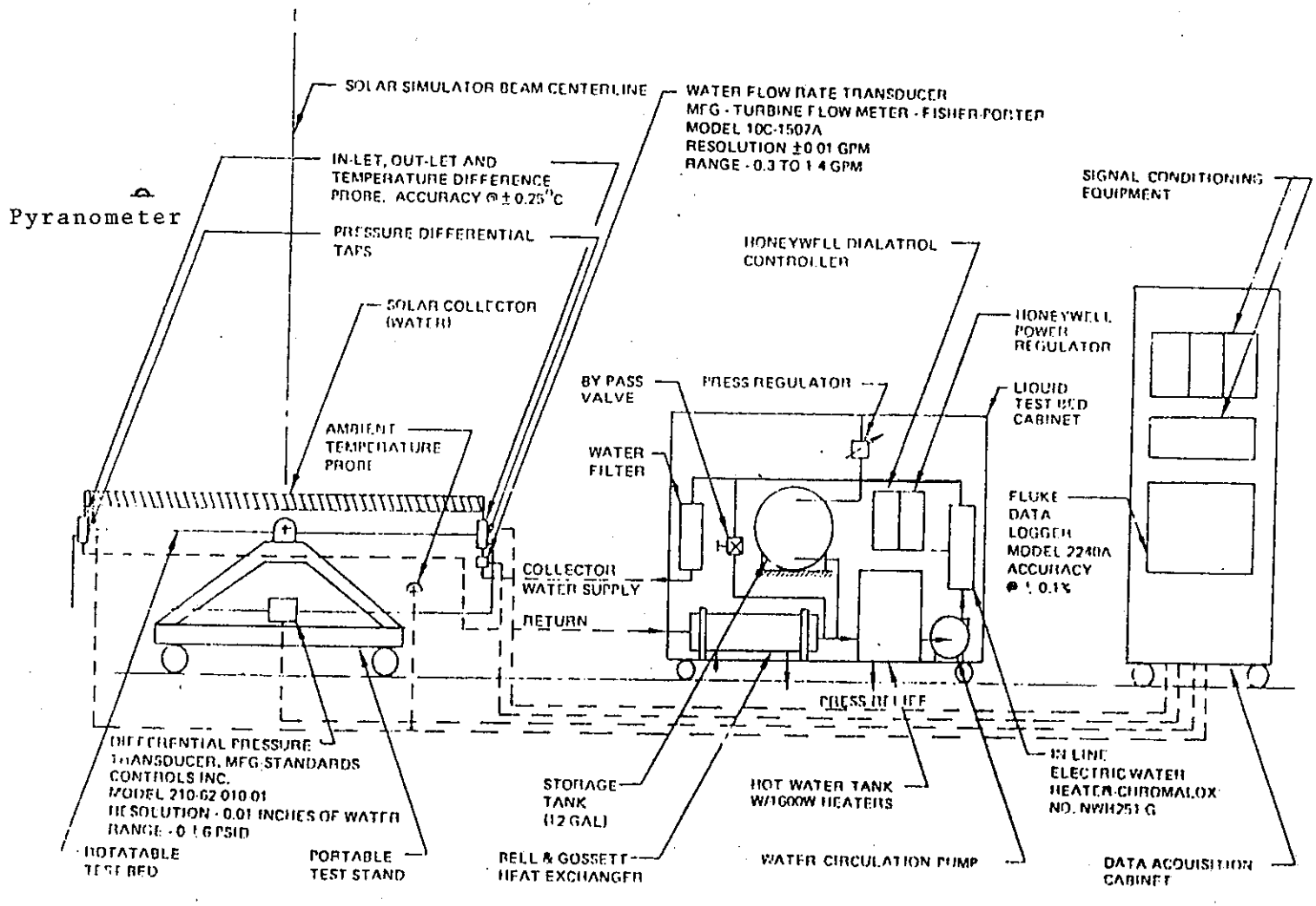

Figure 18 Liquid Test Bed - Schematic

3. DISCUSSION OF SIMULATOR CHARACTERISTICS

Three primary types of simulator were used in the IEA program. Of the seven simulators, two utilize Tungsten-Halogen, two Xenon and three Compact Source Iodine (CSI) lamp sources. Participants 4 and 7 employed Xenon arc simulators primarily designed for AM 0 simulation in space; participant 4 modified the spectrum for AM 2 terrestrial simulation. Participants 1 and 6 used Tungsten Halogen lamps with simulators modelled on the design used at NASA Lewis [7]. Participants 2, 3 and 5 used simulators employing the Compact Source Iodide lamp. With the exception, in some cases, of the number of lamps used the overall simulator designs are similar for those using the same lamp.

The design or selection of a simulator for use in solar collector testing is naturally influenced by the availability of existing facilities, the availability of suitable lamps, and by costs. Simulator specifications have been proposed in both ASHRAE 93 - 77 [4] and AFNOR 77511 [10], (see Appendices 1 and 2) but not all the simulators used in the IEA program were able to meet these specifications. A description of simulation and test requirements for materials testing is published as an international standard but apparently has not been applied to testing solar collectors [11]. Some of the main design features are therefore discussed below.

SPECTRUM

Each of the facilities reported a nominal AM 2 spectrum, but conformity with this spectrum throughout the lifetime of the lamps has not been confirmed for the CSI and Tungsten Halogen lamps. Emission of infra-red radiation from the lamps and lamp housings may be an important characteristic of solar simulators.

BEAM DIVERGENCE

Only Participant 7 was able to meet the ASHRAE 93 - 77 specification (a subtended angle of less than 12 degrees for 95 % of the energy output). Most of the participants reported a half angle of approximately 9° for 90 % of the energy output, but Participant 6 reported a half angle of 12°.

UNIFORMITY

All of the Participants were able to meet the ASHRAE 93-77 specification of ± 1o % of the average intensity, except Participant 2 who reported ± 2o %. Naturally the uniformity is related to the size of the test area used with a given number of lamps, and in general it can be seen from section 12 that the uniformity is best in the simulators with a small test area. The uniformity in simulators with many lamps may vary as lamps reach the end of their lives and the output of new lamps may also be expected to vary from one lamp to another.

VARIATION OF AZIMUTH ANGLE

Participants 5, 6 and 7 have fixed azimuth, Participants 2, 3 and 4 can vary the azimuth as much as they desire by rotating their collector mounting, and Participant 1 can vary the azimuth by ± 6o degrees. No results at other than normal incidence have yet been reported.

VARIATION OF COLLECTOR TILT

All Participants were able to test at a tilt of 45^{o}, except Participant 5 who has a fixed tilt of 22.5^{o} and Participant 7 who tests with a horizontal collector. Participant 6 has a fixed tilt of 45^{o}, but all others can vary their tilt angle.

CLIMATIC CHAMBER

Only Participants 4 and 7 used a climatic chamber.

AIR FLOW ACROSS THE COLLECTOR

All Participants were able to produce an air flow except Participants 6 and 7. Only Participant 2 was unable to achieve the minimum air speed of 3.5 m/s specified by ASHRAE 93-77.

DIFFUSE RADIATION

None of the solar simulators can provide diffuse solar radiation.

4. COLLECTOR TEST PROCEDURE

All Participants having a solar simulator attempted to use the ASHRAE 93 - 77 testing procedure to determine the thermal efficiency of the solar collectors. An appropriate test loop was built indoors where the collectors could be irradiated using a solar simulator. However, not all the simulators used were able to meet the ASHRAE specifications, particularly with regard to spectrum, uniformity, parallelism and artifical wind.

An important difference between the simulators is the instrumentation each employ for measuring incident radiation. In that the instrumentation varies it is anticipated that the method or procedure each follows may also vary. Since detailed descriptions of the irradiance measurement procedures were not available possible measurement errors could not be accessed in this report.

5. DESCRIPTION OF IEA - ROUND ROBIN COLLECTORS

Two commercially available flat-plate liquid-heating collectors were chosen for the tests. It was agreed that one collector should be single glass covered with a selective coated absorber, and the other double glass covered with a flat black painted absorber. The collectors selected for testing were the same as those measured in the outdoor thermal performance and indoor heat loss tests to permit comparison of data taken by the several methods.

The collector coded in this report as the IEA-1 collector had one tempered glass cover of high transmittance, $\tau = 0.90$, the absorber plate was made from steel and was coated with a selective surface ($\alpha = 0.94$; $\varepsilon = 0.12$). Thermal insulation was provided by the mounting block and layers of glass-fibre on the back. The collector box was roll formed and consisted of galvanized steel. A schematic drawing of the collector is shown in Figure 19. A list of collector characteristics and parameters is given in Table 3.

The collector coded in this report as the IEA-2 collector had two float glass covers of a single glass transmittance $\tau = 0.88$. The absorber foil and the tubes were made from copper. The absorber foil was wrapped around the tube covering 75 % of the tube area. The surface was coated with matt black polimerized paint (expected values: $\alpha = 0.95$; $\varepsilon = 0.92$). The absorber was packed by rigid foam polyurethane insulation. The whole system was housed in an aluminium casing. A plan view and cross section view of the collector is shown in Figure 20. A list of collector characteristics and parameters is given in Table 3.

Since it is apparent that replicates of each collector were tested, the question of product variation arises. The collectors used apparently had not been previously tested, therefore no base reference data exists to determine how much variation there may have been from collector to collector.

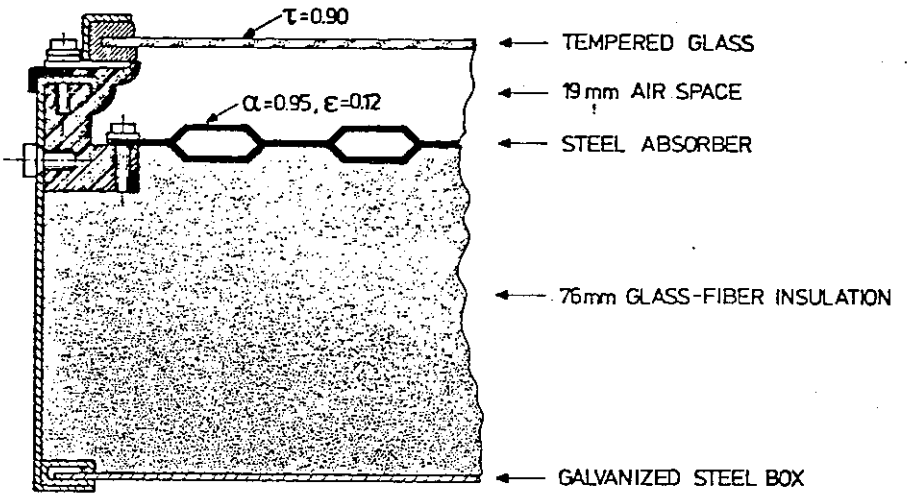

Figure 19 SCHEMATIC OF FLAT-PLATE COLLECTOR IEA-1

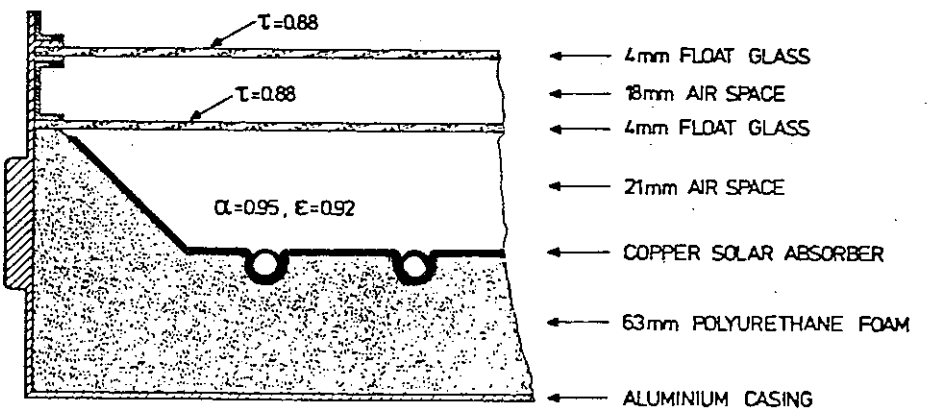

Figure 2o SCHEMATIC OF FLAT-PLATE COLLECTOR IEA-2

6. COLLECTOR PERFORMANCE

The performance of flat-plate collectors is investigated under conditions where essentially no heat is either released or stored by the structure and by the heat transfer medium in it. Effects of geometry can be neglected and the thermal conditions of the collector system can be described by averaged temperatures. The rate of energy extracted from the collector balances the rate of radiative energy absorbed and of heat lost to a uniform environment.
This state may be expressed as:

$$\frac{\dot{Q}_u}{A_a} = G \cdot (\tau\alpha)_e - U_L \cdot (T_p - T_a) \qquad (1)$$

$\dot{Q}_u$ = useful power extracted from the collector (W)
A_a = aperture area of collector (m^2)
G = solar irradiance, in the plane of the collector per unit area ($W \cdot m^{-2}$)
$(\tau\alpha)_e$ = effective transmittance - absorptance product of the cover-absorber system
U_L = heat transfer loss coefficient for the collector ($W \cdot m^{-2} \cdot {}^oC^{-1}$)
T_p = average temperature of the absorber surface of the collector (^oC)
T_a = ambient air temperature (^oC)

Since the plate temperature is difficult to access by measurements, at least by non-destructive test-methods, it is convenient to relate the performance to the temperature of the fluid It was shown by Duffie and Beckmann [6] that either the inlet temperature or a mean temperature can be an appropriate reference temperature. This results in two equations:

$$\frac{\dot{Q}_u}{A_a} = F' \cdot G\,(\tau\alpha)_e - F' \cdot U_L \cdot (T_m - T_a) \qquad (2)$$

$$\frac{\dot{Q}_u}{A_a} = F_R \cdot G\,(\tau\alpha)_e - F_R \cdot U_L \cdot (T_i - T_a) \qquad (3)$$

F' = collector efficiency factor

F_R = collector heat removal factor

T_m = mean temperature of the heat transfer fluid in the collector (arithmetic mean of inlet and outlet temperature for example)

T_i = collector inlet temperature

T_o = collector outlet temperature

Equation (3) is now a feature of the ASHRAE-method, while equation (2) was peculiar to the NBS-method.

The quotient of two energy rates is the collector efficiency η:

$$\eta = \frac{\dot{Q}_u}{A_a \cdot G} = F' \cdot (\tau\alpha)_e - F' \cdot U_L \frac{(T_m - T_a)}{G} \qquad (4)$$

$$\eta = \eta_o - U_m \frac{(T_m - T_a)}{G} \qquad (5)$$

$\eta_o = F' \cdot (\tau\alpha)_e$, Efficiency for $T_m = T_a$

$U_m = F' \cdot U_L$ global heat transfer coefficient ($W.m^{-2}.{}^oC^{-1}$)

If values of η are plotted versus corresponding values of $(T_m - T_a)/G$ this will result in a curve with a negative slope U_m and intercept η_o.

This equation forms the basis of the test procedures.

7. RESULTS AND ANALYSIS OF DATA

A round robin test program using solar simulators was conducted by the International Energy Agency (IEA) with 7 laboratories from different countries (Denmark, Germany, Japan, Sweden, United Kingdom, USA [2x] using the NBS-proposed procedure. Whilst conducting the round robin test programs with the CEC and the IEA, the need for a standard reporting format became obvious. A proposal for a performance test format sheet [9] found general support and was jointly developed to a versatile tool of round robin testing. The results of this round robin test were exclusively reported on this standard format for better data handling.

As a first step the data were subjected to least square fitting to confirm a correct interpretation of the author's results. The format sheets required a fit according to

$$\eta = \eta_o - a_1 \cdot T^* - a_2 \cdot (T^*)^2 \qquad (6)$$

$$T^* = U_o \cdot \frac{(T_m - T_a)}{G}$$

U_o = normalizing coefficient
10 ($W \cdot m^{-2} \cdot {}^oC^{-1}$)

The reference area (Aperture area A_a) determined and reported by the Participants showed no remarkable scatter for both collectors. Due to a maximum test diameter of 1.6 m both collectors were shortened by Participant 4 to an area of approximately 1 m^2. A comparison of thermal efficiency data between the different indoor tests using a solar simulator has been done to determine to what extent the results differed or were comparable. The initial comparison made was for tests on two types of liquid-heating flat-plate collectors, with different optical and heat transfer properties. A description of the IEA round robin collectors and a scheme of the two solar collectors tested was given in para 5.

A plot of the collector efficiency versus $T^* = [U_o (T_m - T_a)/G]$ along with the testing conditions for each of the data points was reported by 7 participants for IEA-collector I (see Figures 25 - 31) and by 5 participants for IEA-collector II (see Figures 32 - 36). The factors for the two collectors, the ordinate intercept and the parameters a_1 and a_2 of the efficiency curve were determined either by the participant or by the author. No attempt was made to correct the data for the difference in test conditions depending partly on the various constructions of the solar simulators and the differences in wind conditions, incident angles or tilt angles and irradiance levels. All indoor solar simulator measurements were performed under 0 % of diffuse radiation.

IEA - Collector I

The indoor instantaneous efficiency curves of IEA collector I derived from 1st or 2nd order least square fits to Participants test results are shown in Figure 21. The curves are only presented for tests using solar simulators. Data points should be determined over the full range of the collector operating conditions because the distribution of the test data points influences the least squares fit of the curve.

Discussion of Results

The relatively large deviation of η_o - values for collector I can only be reduced by eliminating the data of Participant 1 (η_o = 0.985). A possible reason for the large deviation of Participant 1 might be the difference between the spectral distribution of the solar simulator and the solar irradiance. Participant 1 has no precise instrument available to measure the spectral distribution of the irradiated energy.

The other 6 Participants obtained η_o- values between 0.833 and 0.878 or - 2.6% and + 2.7%. The conversion factors η_o obtained from the test results of each Participant are presented in Figure 22 for IEA-collector I. The average value (excluding Participant 1) of the conversion factor η_o was calculated to be $\overline{\eta}_o$ = 0.855. The standard deviation is in the range of $\sigma = \pm$ 0.018.

The results and analysis of a round robin test program in the US for the same liquid-heating flat-plate solar collector are shown in [3]. The average value of the conversion factor measured by 21 Participants was calculated to be $\overline{\eta}_o$= 0.84. The standard deviation was in the range of $\sigma = \pm$ o.o36. Seven test facilities that conducted the tests in accordance with the ASHRAE Standard 93-77 requirements, the average values for the intercept and slope for a linear fit equation were o.844 and 4.69, respectively with a standard deviation of o.o18 for the intercept and o.o79 for the slope. The overall reproducibility of the simulators, while better than the 21 facilities in the outdoor round-robin,

appears to be about the same as the results obtained from those outdoor facilities in that round robin that met ASHRAE 93-77 requirements.

If the collector I data of Participant 1 are neglected because they deviate so far from the others, then the mean values of the conversion factors and the slopes of the curves have an acceptable scatter. The range of environmental conditions, especially the wind velocities of 0 to 8 $m \cdot sec^{-1}$ during the tests at the various facilities could partially account for the data scatter.

The collector tends to require a higher order fit in the analysis. The intercepts η_o are usually lower for a second-order fit.

A summary of the test results as intercepts η_o, slopes or coefficients of the efficiency curves is given in Table 4.

The differences in the collector thermal characteristics deduced in the round robin tests are attributed to the various designs of the solar simulators, the environmental conditions, the experimental uncertainties and possible systematic errors.
A comparison of the curves and the mean conversion factor $\overline{\eta}_o$ for all outdoor and all indoor solar simulator measurements is additionally given in Figures 21 and 22. The mean conversion factor $\overline{\eta}_o$ measured indoors (η_o= o.855) is 3% higher than that measured outdoors ($\overline{\eta}_o$ = o.83) probably due to lower wind velocities during indoor measurements. The standard deviation $\sigma = \pm$ o.o18 is lower for indoor data than for the outdoor data ($\sigma = \pm$ o.o3).

The mean value of the slopes of the efficiency curves measured indoors with the solar simulators was o.5o6 and the standard deviation ± o.o49 or 9.6% (see Table 4).

IEA - Collector II

The indoor instantaneous efficiency curves of IEA collector II derived from 1st or 2nd order least square fits to Participants' test results are presented in Figure 23. Only 5 participants have performed collector II tests using a solar simulator. Data points should be determined over the full range of the collector operating conditions because the distribution of the test data points influences the least squares fit of the curve.

Discussion of Results

The conversion factors η_o of the 5 participants (1,2,3,4,7) are in the range of 0.555 to 0.616 or - 6.6% to + 3.7%. The conversion factors η_o obtained from the test results of each participant are presented in Figure 24 for IEA-collector II. The average value of the conversion factor η_o was calculated to be $\overline{\eta}_o = 0.594$.

The standard deviation is in the range of $\sigma = \pm 0.025$. The mean values of the conversion factors and the slopes of the curves have an acceptable data scatter. The range of environmental conditions during the tests at the various facilities could partially account for the data scatter.

For this collector a linear fit seems to be sufficient. The intercepts η_o are usually higher for a linear fit. A summary of the test results as intercepts η_o, slopes or coefficients of the efficiency curves is given in Table 5.

A comparison of the curves and the mean conversion factor for all outdoor and all indoor solar simulator measurements is additionally given in Figure 23 and 24. The mean conversion factor $\overline{\eta}_o$ measured indoors ($\overline{\eta}_o = 0.594$) is about 4,2% higher than that measured outdoors ($\overline{\eta}_o = 0.57$). The standard devitation σ is lower for indoor ($\sigma = \pm 0.025$) than for outdoor data (NBS: $\sigma = \pm 0.05$; BSE: $\sigma = \pm 0.04$). The mean value of the slopes of the efficiency curves measured indoors was calculated to be 0.436 with a standard deviation of $\pm$ 0.038 or 8.7% (see Table 5). The outdoor value was 0.43 with a standard deviation of $\pm$ 0.094 or 21.9%.

8. CONCLUSIONS

The results obtained in the solar simulators were in close agreement with those obtained outdoors. The values of η_o obtained in the simulators were slightly higher, but this can probably be attributed to unrepresentative simulation of diffuse solar radiation, effective temperature, environment temperature, and wind speed in the simulators.

It has been shown that simulators representing a wide range of the state of the art in sophistication can produce good collector test results on the collectors tested. Since some of the simulators have characteristics which fall outside the range required by ASHRAE 93 - 77, the extent to which outdoor conditions must be faithfully reproduced has yet to be confirmed. Furthermore the need for faithful reproduction of outdoor conditions may be expected to vary from one collector to another. For example the need for parallelism will be greater with concentrating collectors and that for uniformity will be greater when testing collectors which are unable to integrate the energy input over their collection area.

The use of solar simulators is very attractive to laboratories in parts of the world where clear days are infrequent. In particular, simulators are favoured by countries in Northern Europe where there are few days in the year which can meet AHSRAE 93-77 outdoor requirements.

With only a few exceptions, the simulators show good promise to potentially provide test results that are both reproducible and correlate well to outdoor performance.

9. FUTURE WORK PROPOSED IN THE FIELD OF SOLAR SIMULATORS

Solar simulator test facilities used for collector testing should have suitable characteristics with respect to the spectral distribution of the irradiance, the uniformity of the irradiance, the size of the irradiated area, the variation of the incident angle and the effective environment parameters. Differences in results seem to be associated more with simulator design, control/conditioning apparatus design and operational procedure rather than environmental test conditions.

Therefore future work should result in identifying simulator characteristics more precisely. The test procedure also needs to be evaluated. Such items as measurement of uniformity, background radiation, ambient temperature, spectral distribution, collimation angle, and the test conditions (flow, tilt, wind, and fluid temperature) must be specified as currently in the existing test procedures or added as necessary. Evaluation test programs for simulators must include a variety of collector types and materials to demonstrate that the simulator is adequate for a broad class of collectors or to establish limitations and possible corrections required for their use in order to achieve test results comparable to those obtained outdoors.

The future work proposed has to be seen in the light of the recent development to use cheaper simulators for collector testing. For the design of a cheap simulator the necessary characteristics have yet to be determined.

Depending on the results from the identification of simulator characteristics, selective tests should be considered using a single collector whose performance characteristics are well established. A group of collectors can be used only if they are all tested thoroughly before any round-robin or other tests such that any variation between collectors is quantified.

10. NOMENCLATURE [12]

Symbol	Meaning	Units
a_o, a_1, a_2	Algebraic constants	-
A_a	Aperture area of collector	m^2
A_g	Gross area of collector	m^2
A_p	Absorber plate area of collector	m^2
c_f	Specific heat of heat transfer fluid	$J\ kg^{-1}\ K^{-1}$
C	Effective thermal capacity of collector	$J\ K^{-1}$
$C_{t\ell}$	Effective thermal capacity of test loop	$J\ K^{-1}$
D	Date	Day-Month-Year
E	Voltage output	Volts
e	Error of curve fit	Dimensionless
G	Solar and shortwave irradiance	$W\ m^{-2}$
G_d	Diffuse solar irradiance	$W\ m^{-2}$
$K(\theta)$	Angle of incidence modifier	Dimensionless
$\dot{M}$	Mass flow of heat transfer fluid	$kg\ s^{-1}$
N	Number of data points	Dimensionless
P	Electrical Power Input	W
$\dot{Q}_\ell$	Power loss of the collector	W
$\dot{Q}_T$	Total power collection of the collector	W
$\dot{Q}_u$	Useful power extracted from the collector	W
R_o	Thermometer resistance at 273K	Ω
R_T	Thermometer resistance at temperature T	Ω

Symbol	Meaning	Units
T	Absolute temperature	K
T_a	Ambient air temperature	K
T_e	Collector outlet temperature	K
T_i	Collector inlet temperature	K
T_m	Mean temperature of the heat transfer fluid	K
T_A	Atmospheric or sky equivalent radiation temperature	K
T^*	Reduced temperature	Dimensionless
U_o	Normalized heat transfer coefficient	$U_o = 10\ Wm^{-2}K^{-1}$
U_m	Overall heat transfer coefficient	$Wm^{-2}K^{-1}$
$U_{t\ell}$	Overall heat loss of the test loop	$W\ K^{-1}$
u_s	Surrounding air speed	$m\ s^{-1}$
η	Collector efficiency	Dimensionless
η_o	Conversion factor (η at $T^* = 0$)	Dimensionless
$\bar{\eta}_o$	Mean value of the measured conversion factors	Dimensionless
Δp	Pressure difference of the fluid between inlet and outlet	Pa
ΔT	Temperature difference of the fluid between inlet and outlet	K
Θ	Angle of incidence of direct solar radiation	Degress
σ_e	Standard error of the curve fit	-

11. REFERENCES

[1] Hill, J.E.; Kusuda, T.
Method of Testing for Rating Solar Collectors Based on Thermal Performance
NBSIR 74-635, December 1974, Washington, D.C.

[2] Usability of Solar Collectors, Guidelines and Directions
A Solar Collector Efficiency Test
BSE, 4300 Essen, Germany, May 1978

[3] Streed, E.R.; Thomas, W. C.; Dawson, K. G.; Wood, B.D. and Hill, J.E.
Results and Analysis of a Round Robin Test Program for Liquid-heating Flat-Plate Solar Collectors
NBS-Technical Note 975, August 1978, Washington, D.C.

[4] Methods of Testing to Determine the Thermal Performance of Solar Collectors
ASHRAE Standard 93-77,
ASHRAE, 345 East 47th Street, New York, N.Y. 10017, 1977

[5] Ramsey, J.W.; Borzoni, J.T. and Holland, T.H.
Development of Flat-Plate Solar Collectors for the Heating and Cooling of Buildings
NASA CR-134804, June 1975

[6] Duffie, J.A. and Beckmann, W.A.
Solar Energy Thermal Process, John Wiley and Sons,
New York, 1974

[7] Simon, F.F.
Comparison under a simulated Sun of two Black-Nickel-Coated Flat-Plate Solar Collectors with a Nonselective Black-Paint-Coated Collector
NASA TM X - 3226, June 1975

[8] Simon, F.F.
An experimental Investigation with artificial Sunlight of a Solar Hot-Water Heater
Joint Conference of the International Solar Energy Society and the Solar Energy Society of Canada
Winnipeg/Canada, August 1976

[9] Aranovitch, E.
Proposal on: Performance Tests Format Sheets Solar Collector Testing Programme
European Commission Joint Research Centre, Euratom
ISPRA/ITALY, 1977

[10] AFNOR P 50-501
Capteurs Solaires-Mesure des Performances Thermiques
AFNOR 77511, Dec. 1977

[11] NBSIR - 77 - 1314
Solar Energy Systems-Survey of Materials Performance

[12] Derrik, A.
Recommendations for European Solar Collector Test Methods
Solar Energy Unit, University College, Cardiff, U.K.

[13] Hottel, H.C.; Woertz, B.B.
The Performance of Flat-Plate Solar Heat Collectors
ASME-Transactions, Vol. 64, 1942

[14] Tabor, H.
Selective Surfaces for Solar Collectors
Chapter VI in "Applications of Solar Energy for Heating and Cooling of Buildings"
ASHRAE, New York, 1977

[15] Yass, K.; Curtis, H.B.
Low-Cost Air Mass 2 Solar Simulator
NASA TM X-3059, October 1973

[16] Simon, F.F.; Harlamert, P.
Flat-Plate Collector Performance Evaluation, the Case for a Solar Simulator Approach
NASA TM X-71427

2. TABLES AND FIGURES

Key to Participants	1
Researcher and Institution	Solar Research Laboratory/Showa Aluminium Co. Nagoya/Japan — Oyama/Japan S. Tanemura — A. Okamoto
Simulator operating	yes
Lamps Source	General Electric ELH 300 W, Tungsten Halogen
Number of Lamps	187
Lifetime of Lamps	80 h
Maximum Irradiance	1100 W . m^{-2}
Variation of Irradiance	500 ÷ 1100 W . m^{-2}
Test Area	1.2 x 1.8 m^2
Spectrum	AM2
Divergence, half angle	4.5°
Uniformity	± 5 %
Variation of Azimuth Angle	possible by rotating the simulator up to 60 deg.
Variation of Tilt Angle	possible
Climatic Chamber	no
Wind	0 ÷ 5 m . sec^{-1}

Table: 1 Status of Solar Simulators

Key to Participants	2	3
Researcher and Institution	University College Cardiff, UK W.B. Gillett	Statens Provningsanstalt Boras/Sweden H.E.B. Anderson
Simulator operating	yes	yes
Lamps Source	Compact Source Iodide Lamps Thorn Ltd., UK 1 kW each	Compact Source Iodide Lamps, Thorn Ltd., UK 1 kW each
Number of Lamps	19	36
Lifetime of Lamps	1000 h	1000 h
Maximum Irradiance	900 W . m^{-2}	1100 W . m^{-2}
Variation of Irradiance	400 ÷ 900 W . m^{-2}	200 ÷ 1100 W . m^{-2}
Test area	2.25 m Ø	2 x 2 m^2
Spectrum	AM2	AM2
Divergence, half angle	9° to 1o% power	4.5° to half power
Uniformity	± 20 %	±10 % without individual regulation of each lamp
Variation of Azimuth Angle	possible by rotating the collector mounting	possible by rotating the test device
Variation of Tilt Angle	vertical to horizontal	vertical to horizontal
Climatic Chamber	no	no
Wind	less than 2 m . sec^{-1}	0 ÷ 10 m . sec^{-1}

Key to Participants	4	5
Researcher and Institution	DFVLR, Cologne/Germany W. Ley	Technical University of Denmark Lyngby/Denmark S. Svendsen
Simulator operating	yes	yes
Lamps Source	Osram or Philips 6.5 kW each	Compact Source Iodide Lamps 1 kW each
Number of Lamps	10	36
Lifetime of Lamps	600 h	1000 h
Maximum Irradiance	1700 $W \cdot m^{-2}$	1200 $W \cdot m^{-2}$
Variation of Irradiance	100 ÷ 1700 $W \cdot m^{-2}$	1000 ÷ 1200 $W \cdot m^{-2}$
Test area	1.6 m Ø	1.2 x 2.4 m
Spectrum	AM0 or AM2	AM2
Divergence, half angle	9°	9° for a single lamp, 25° for radiation on test area
Uniformity	± 4 %	± 10 %
Variation of Azimuth Angle	possible by rotating the test device	0°, fixed*
Variation of Tilt Angle	possible by tilting of test device	22.5°, fixed*
Climatic Chamber	yes	no
Wind	0 ÷ 10 $m \cdot sec^{-1}$	0 ÷ 10 $m \cdot sec^{-1}$

* Changes decrease uniformity

Key to Participants	6	7
Researcher and Institution	NBS Washington/USA E. Streed	NBS Washington/USA E. Streed
	Honeywell Research Facility* Minneapolis, Minnesota J. D. Kopecky	Boeing Aerospace Seattle/Washington A. R. Lundy
Simulator operating	yes	yes
Lamps Source	General Elec.Co., Model ELH 300 W Tungsten-Halogen	Durotest or ITT 20 kW - Xenon short arc
Number of Lamps	200	7
Lifetime of Lamps	80 h	500 - 1000 h
Maximum Irradiance	1460 W . m^{-2}	2950 W . m^{-2}
Variation of Irradiance	500 ÷ 1460 W . m^{-2}	135 ÷ 2950 W . m^{-2}
Test area	1.6 m^2	7.0 m^2
Spectrum	AM2	AM0 or AM2
Divergence, half angle	12^o	1.75^o
Uniformity	± 8 %	± 10 %
Variation of Azimuth Angle	0	0 (vertical beam)
Variation of Tilt Angle	0 (nominal 45^o tilt)	0 (vertical beam)
Climatic Chamber	no	yes
Wind		

* A similar type of simulator exists at the NASA Marshall Space Flight Center, Huntsville/Alabama which uses 405 lamps to irradiate a test area of 3.1 m^2.

Key to Participants	1	2
Instrumentation		
Incident radiation	Pyranometer EKO-MS4	Kipp & Zonen Solarimeter + chart recorder
Fluid mass flow	OVAL INSTR. INDUST. CO Type 17 micro volume flow meter of a pulse generating type with an accuracy of ± 5 %	Rotameter, Manual Record + temp. correction
Ambient temperature	Cu-Const. thermocouple with an accuracy of ± 0.2° C	Shaded mercury in glass thermometer
Fluid absolute temperature	ditto	Cr/Al thermocouples + electronic thermometer
Differential fluid temperature	not directly measured	3 x 3 Cr/Al thermopile + chart recorder
Wind velocity	Anemometer using a thermistor as the sensor with an accuracy of $\pm$ 0.2 m . sec^{-1}	Vane anemometer at panel mid-height
Data recording	Multi-channel digital thermorecorder with 30 sec sampling intervals	Manual with 2-Pen recorder for I & T

Table 2: Instrumentation

Key to Participants	3	4	5	7
Instrumentation				
Incident radiation	Eppley precision pyranometer LI-COR, Lambda Instruments Corp.: LI-200 S pyranometer	Kendall Mark IV radiometer	Eppley precision spectral pyranometer	Eppley pyranometer Model PSP
Fluid mass flow	Turbine flowmeter Flow Technology Inc.	Mag-Flux-Turbo-meßtechnik	Ringpistonmeter Aqua Metro	Fisher-Porter, water flow rate transducer Model 10 C-1507 A
Ambient temperature	Thermocouple type T	Cu-Const. thermocouple	Cu-Const. thermo-couple	Cu-Const. thermo-couple
Fluid absolute temperature	Pt-100 resistance thermometer	Pt-100 resistance thermometer	Cu-Const. thermo-couple	Water temperature probe, Type K-sheathed thermocouple
Differential fluid temperature	Pt-100 resistance thermometer	Pt-100 resistance thermometer	Thermopile with 10 elements of Cu-Const.	
Wind velocity	Hot wire anenometer	Hoentzsch "Exact-mini-air"	Hot wire anenometer	Alnor velometer Type 3002
Data recording	Scanner HP 3495 A, voltmeter Fluke 8800 A Desk computer HP 9825	Hewlett Packard	Chart recorders, Kipp & Zonen Bd 9	Fluke Data logger, Model 2240 A

Characteristics	Collector IEA-I	Collector IEA-II
1.1 Manufacturer	Chamberlain Mtg.Co, Elmhurst, Illinois USA	Commercial Solar Energy, Nottingham, UK
1.1.1 Date of tests	1978	1977 - 79
1.1.2 Type of collector	flat plate	flat plate
1.2 Transparent covers		
1.2.1 Number	1	2
1.2.2 Thickness (mm)	3.2	4.0
1.2.3 Material	low-iron tempered glass	float glass
1.2.4 Solar transmission (single glass)	0.90	0.88 each
1.2.5 I.R. emittance	0.88	0.88
1.2.6 Aperture dimensions (m)	0.86 x 2.08	1.18 x 1.94
1.2.7 Aperture area (m^2)	1.79	2.29
1.2.8 Air space between cover and absorber (mm)	19.0	21.0
1.2.9 Air space between covers (mm)	-	18.0
1.3 Absorber plate		
1.3.1 Material	mild steel	copper foil
1.3.2 Surface treatment	selective black chrome	matt black paint
1.3.3 Manufacturing process	stitch welded	copper foil clamped to copper tubes
1.3.4 Weight empty (kg)	72.5	67 - 72
1.3.5 Water content (kg)	2.6/3.3	2.5 - 2.6
1.3.6 Dimensions (m)		
1.3.7 Thickness of plate (mm)		
1.3.8 Solar absorptance	0.94	0.95
1.3.9 Solar emittance	0.12	0.92
1.3.10 Absorber constr.	19 parallel pass	10 parallel tubes
1.3.11 Tube spacing (m)	-	0.112

Characteristics	Collector IEA-I	Collector IEA-II
1.4 Thermal insulation		
1.4.1 Thickness (mm)	76.2	50
1.4.2 Material	glass-fibre	polyurethane
1.4.3 Density (kg/m^3)	80	50
1.4.4 Thermal conductivity (W/m . K)	0.03	0.024
1.5 Casing		
1.5.1 Gross dimensions (m)	0.92 x 2.14	1.22 x 2.00
1.5.2 Gross area (m^2)	1.97	2.44
1.5.3 Weight per gross area (kg/m^2)	37.0	
1.5.4 Material	aluminium	aluminium
1.5.5 Thickness (mm)	1	1

Table 3 Description of Solar Collectors Tested
(from manufacturers literature and from [3])

Participant	Linear Curve*				$y=\eta_o-a_1 \cdot T^*-a_2 \cdot (T^*)^2$				A_a m^2	G $W \cdot m^{-2}$	T_a ^oC	u $m \cdot sec^{-1}$	$\dot{M}/A_a$ $g \cdot sec^{-1} \cdot m^{-2}$
	η_o	$\Delta\eta_o$	a_1	Δa_1	η_o	$\Delta\eta_o$	a_1	a_2					
1	[o,992	+13,8 %	o,595	+ 17,6 %]	[o,985	15,2 %	o,556	o,o367]*	1,79	8o5	22	2.48	≈ 2o
2	o,864	- o,9 %	o,532	+ 5,1 %	o,855	o %	o,459	o,1o5	1,78	8oo	2o	2÷4	≈ 19
3	o,858	- 1,6 %	o,571	+ 12,9 %	o,849	- o,7 %	o,47o	o,156	1,78	97o	23		≈ 35
4	o,913	+ 4,7 %	o,49o	- 3,2 %	o,878	2,7 %	o,3o2	o,166	1,o7o6	6oo	15	o	≈ 14
	[o,894	+ 2,5 %	o,495	- 2,2 %]	[o,877	2,6 %	o,375	o,143]*	1,o7o6	9oo	15	o	≈ 14
5	o,848	- 2,8 %	o,522	+ 3,2 %	o,84o	- 1,8 %	o,411	o,161	1,78	917	24	5÷8	≈ 34
6	o,874	+ o,2 %	o,427	- 15,6 %	o,874	2,2 %	o,427	o,o	1,78	66o	2o,4	o	
7	o,874	+ o,2 %	o,494	- 2,4 %	o,833	- 2,6 %	o,2o1	o,424	1,79	1ooo	22÷25	o	≈ 24
Mean	$\bar{\eta}_o$= o,872		o,5o6		$\bar{\eta}_o$= o,855		o,378	o,169					
Standard Deviation	± o,o22		± o,o49		± o,o18								
% Deviation	2,523		9,6		2,1o5								

Table 4 Summary of Collector Thermal Performance
Collector: IEA-I
*Data not used for evaluation

Participant	Linear Curve*				$y = \eta_o - a_1 \cdot T^* - a_2 \cdot (T^*)^2$				A_a m^2	G $W \cdot m^{-2}$	T_a ^oC	u $m.sec^{-1}$	$\dot{M}/Aa$ $g.sec^{-1}.m^{-2}$
	η_o	$\Delta\eta_o$	a_1	Δa_1	η_o	$\Delta\eta_o$	a_1	a_2					
1	o,627	+ 4,7 %	o,442	+ 1,4 %	o,616	3,7 %	o,378	o,o637	2,279	≈ 82o	≈22	2.48	≈ 2o
2	o,611	+ 2,o %	o,383	-12,2 %	o,61o$^+$	2,7 %	o,349$^+$	o,o57$^+$	2,318				
3	o,563	- 6,o %	o,489	+12,2 %	o,555$^+$	-6,6 %	o,391$^+$	o,155$^+$		≈ 1ooo	≈24		≈ 46
4	o,589	- 1,6 %	o,428	- 1,8 %	o,5829	-1,8 %	o,39o4	o,o295	1,o46	6oo/9oo	≈15	o	≈ 14
7	o,6o3	+ o,7 %	o,437	+ o,2 %	o,6o67$^+$	2,1 %	o,574$^+$	o,oo5$^+$					
Mean	$\bar{\eta}_o$ = o,599		o,436		$\bar{\eta}_o$ = o,594		o,417	o,o62					
Standard Deviation	± o,o24		± o,o38		± o,o25								
% Deviation	4,o37		8,672		4,2o9								

Table 5 Summary of Collector Thermal Performance
Collector: IEA - II

$^+$Data recalculated from curve or test data

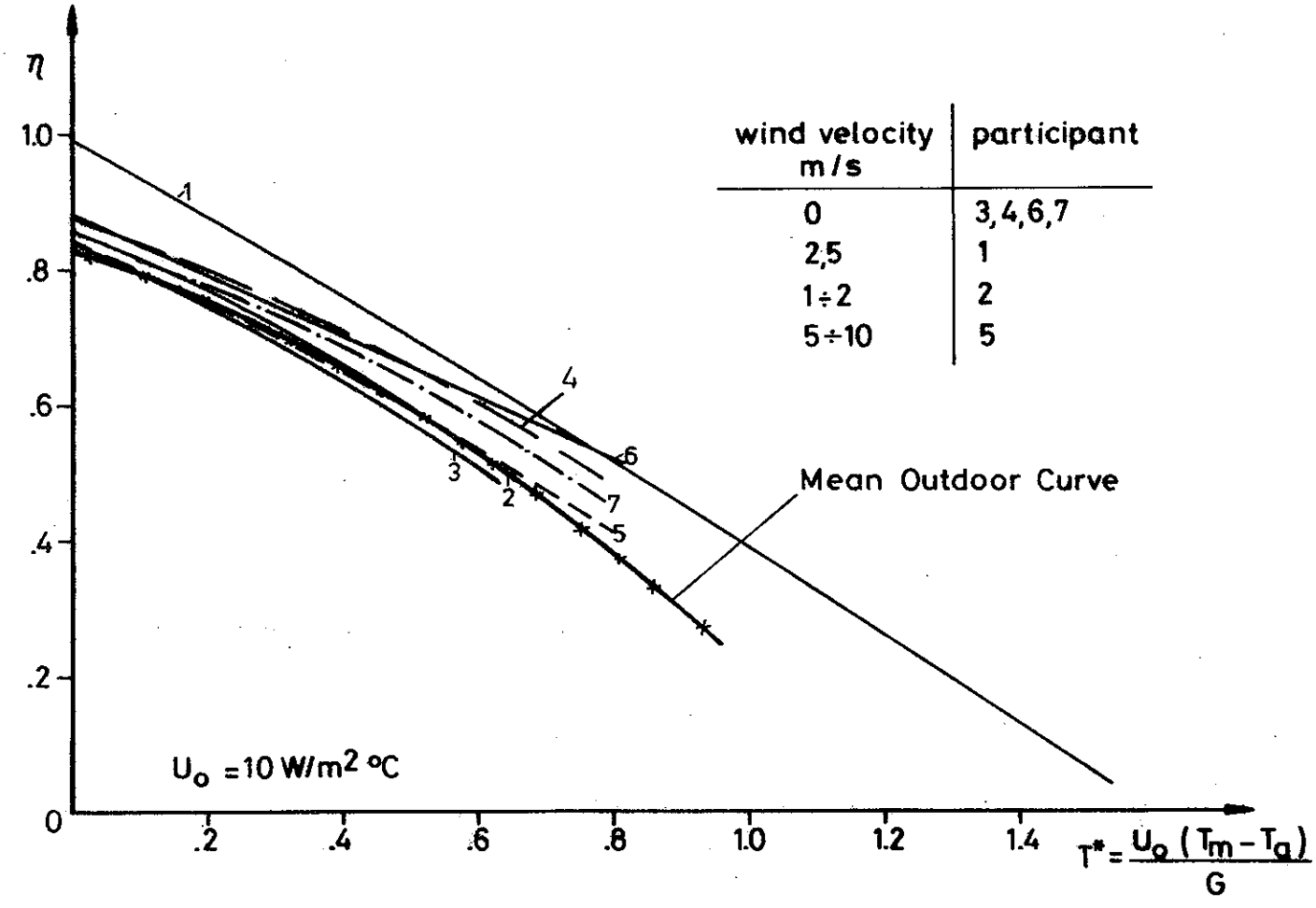

Fig. 21 Indoor Instantaneous Efficiency Curve IEA I

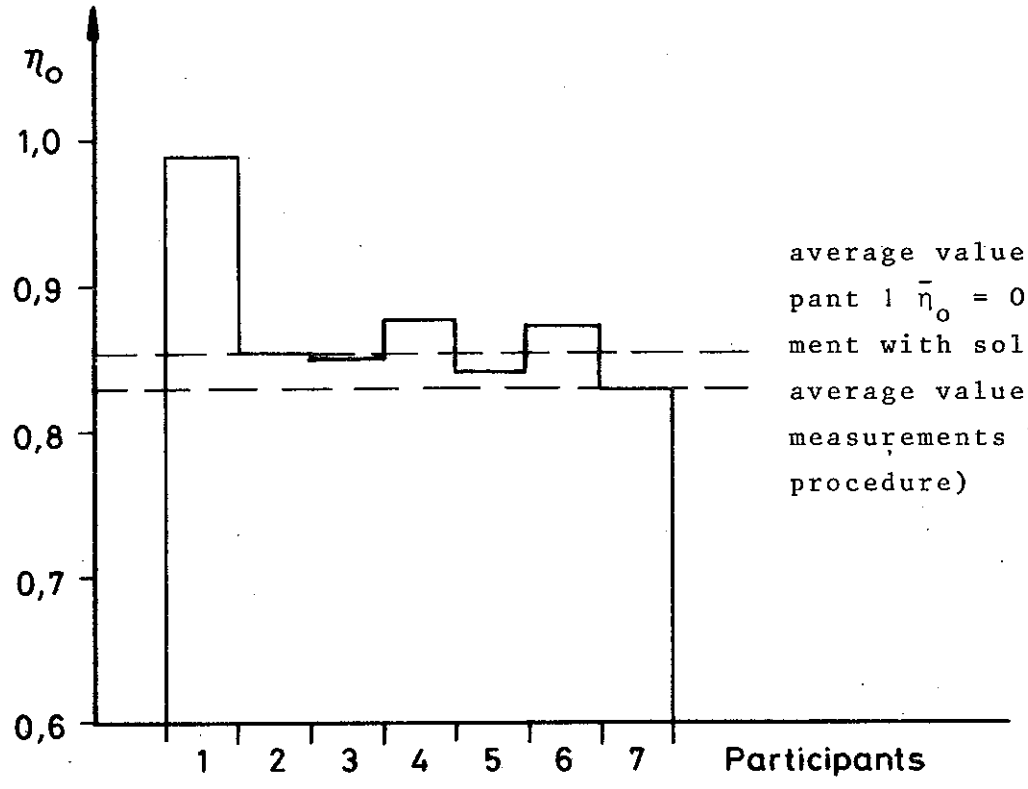

Fig. 22 Conversion Factor η_o Results Indoor IEA I

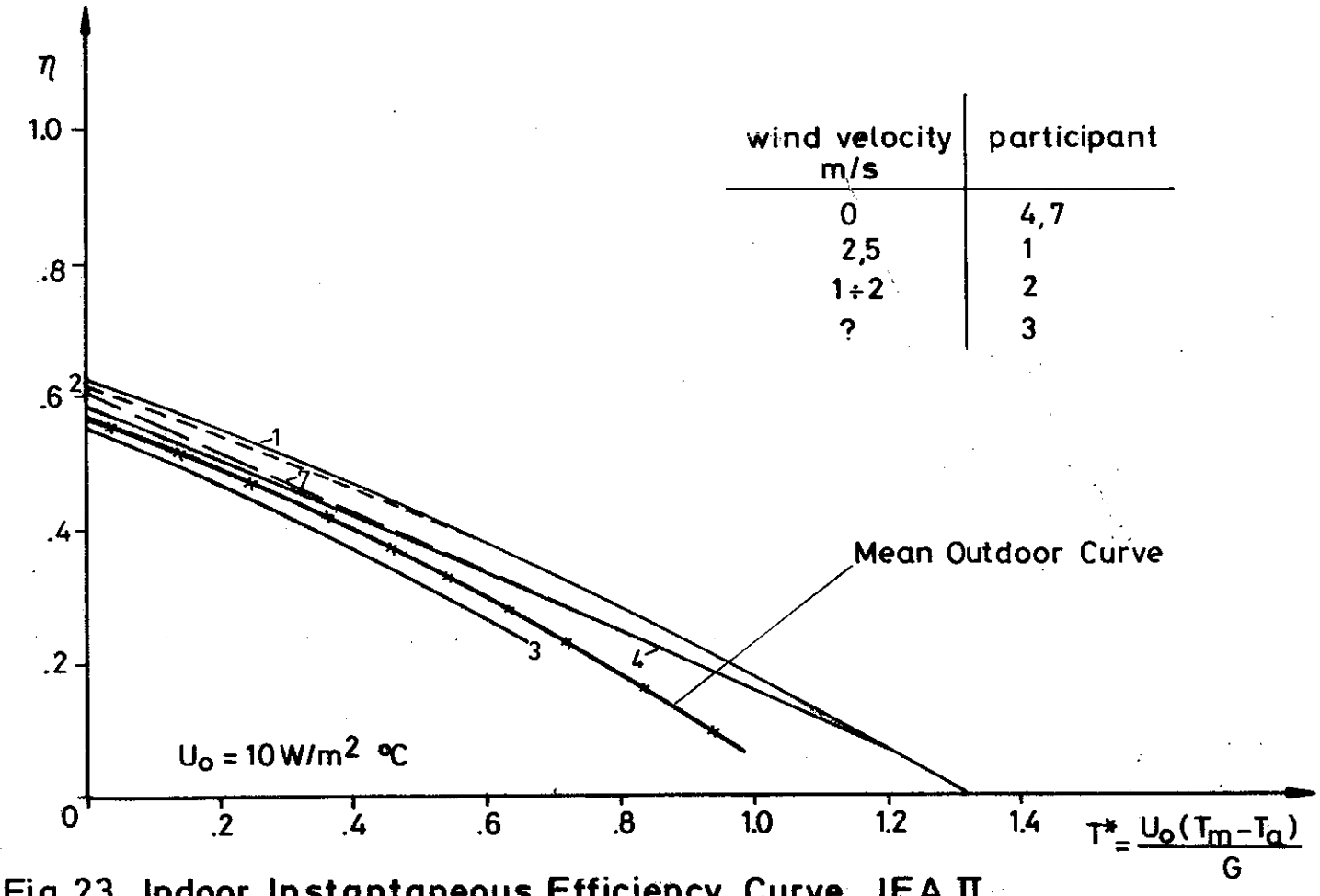

Fig. 23 Indoor Instantaneous Efficiency Curve IEA II

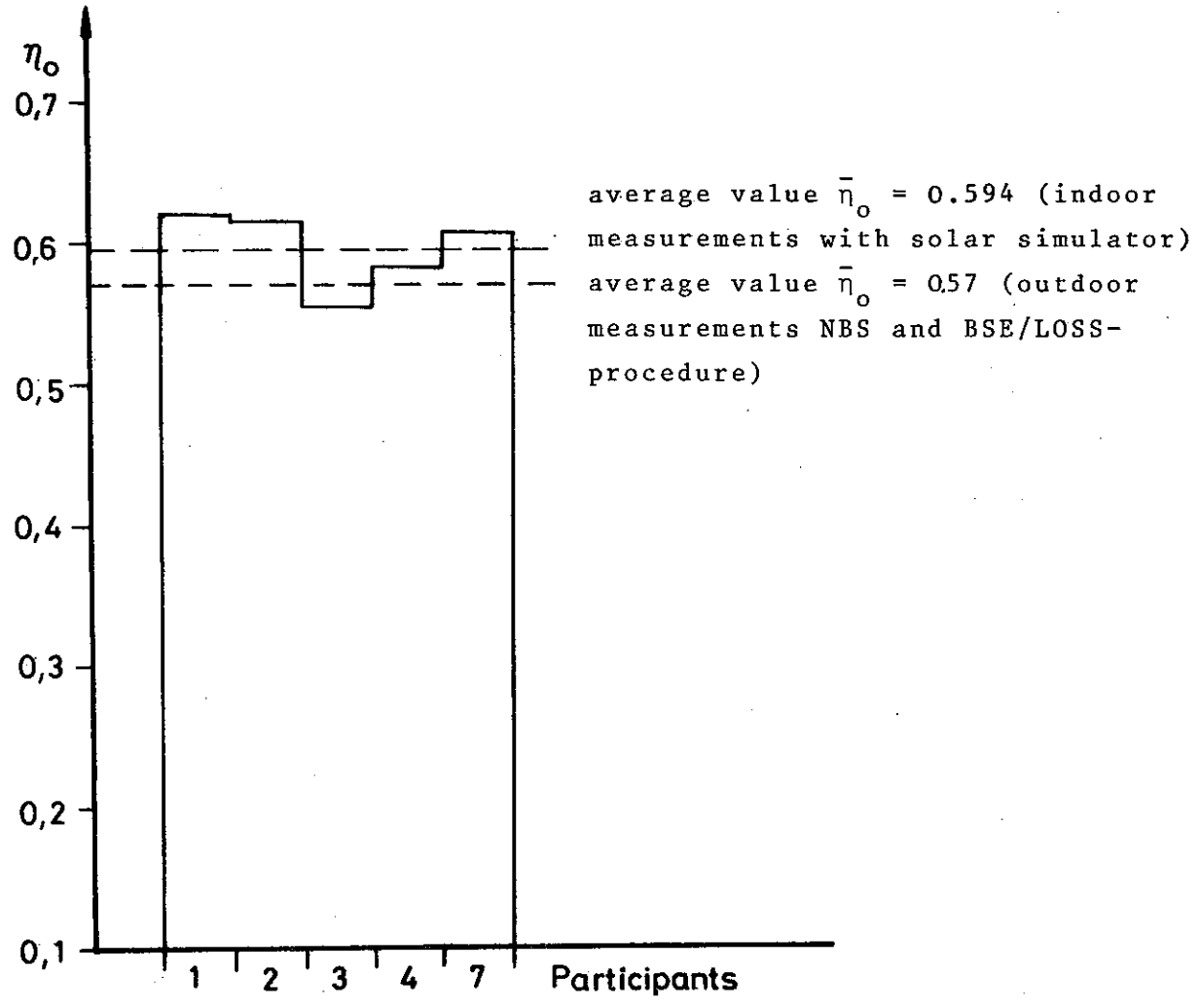

Fig. 24 Conversion Factor η_o Results Indoor IEA II

Test Institute: 1 Collector IEA-I

Instantaneous Efficiency Curve

THE INSTANTANEOUS EFFICIENCY η IS DEFINED BY: $\eta = \frac{\dot{Q}_u}{A_a \cdot G}$

$\dot{Q}_u$: useful power extracted	0	W
G : incident radiation	0	W/m^2
A : reference area	X	m^2 1,79

Specify which area is used for curve:

- 0 gross area of collector
- X aperture area
- 0 absorber area

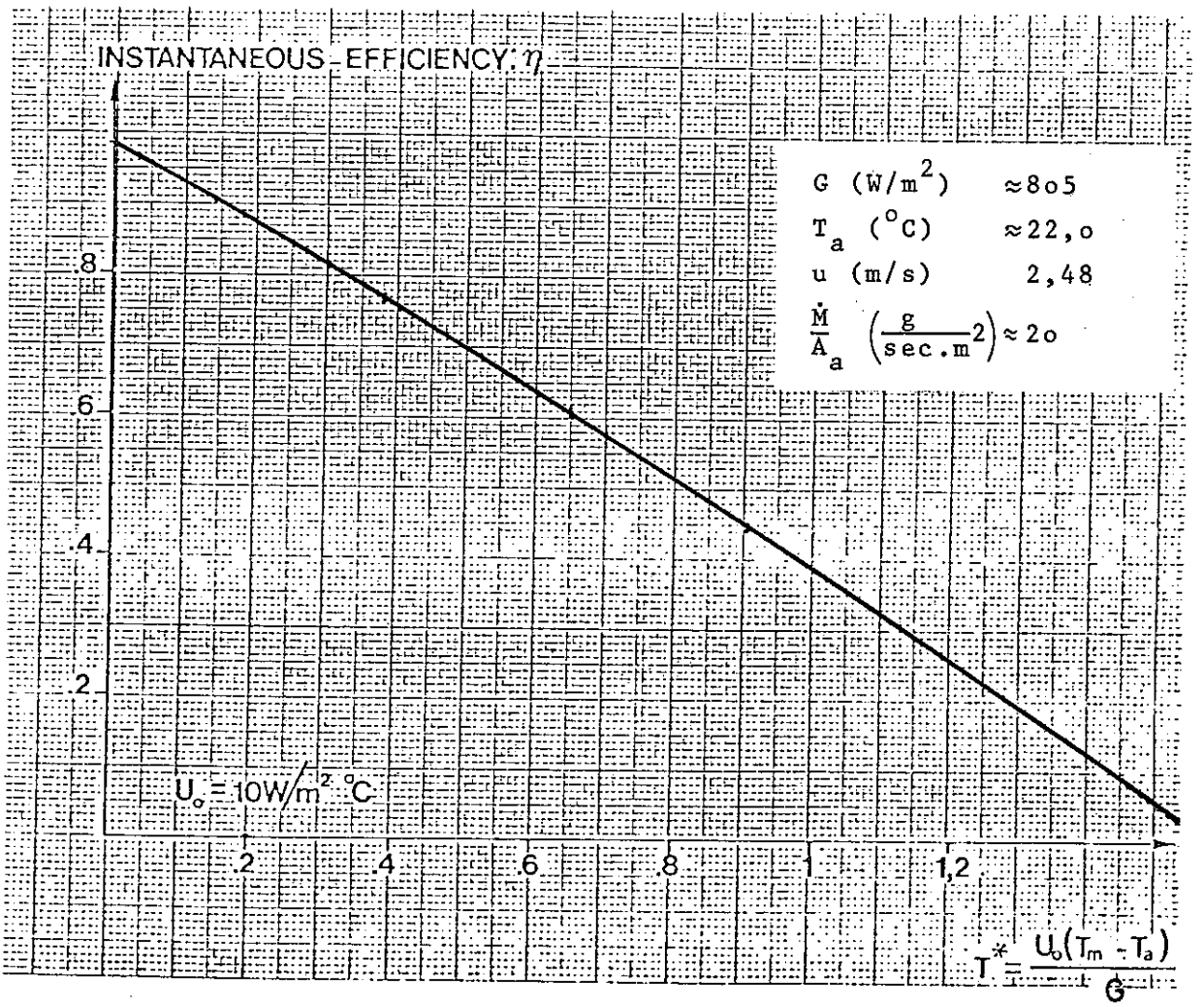

Fig. 25

RECOMMENDED EQUATION: $\eta = \eta_0 - a_1 T^* - a_2 (T^*)^2$

$\eta = 0.98_5 - 0.55_6 T^* - 0.036_7 T^{*2}$ (2nd order)

and

$0.99_2 - 0.59_5 T^*$ (linear)

Test Institute: 2 Collector IEA-I
Instantaneous Efficiency Curve

THE INSTANTANEOUS EFFICIENCY η IS DEFINED BY : $\eta = \frac{\dot{Q}_u}{A_a \cdot G}$

q_u	: useful power extracted	☐	W	
I	: incident radiation	☒	W/m^2	800
A	: reference area	☒	m^2	1.78

Specify which area is used for curve:
- ☐ gross area of collector
- ☒ aperture area
- ☐ absorber area

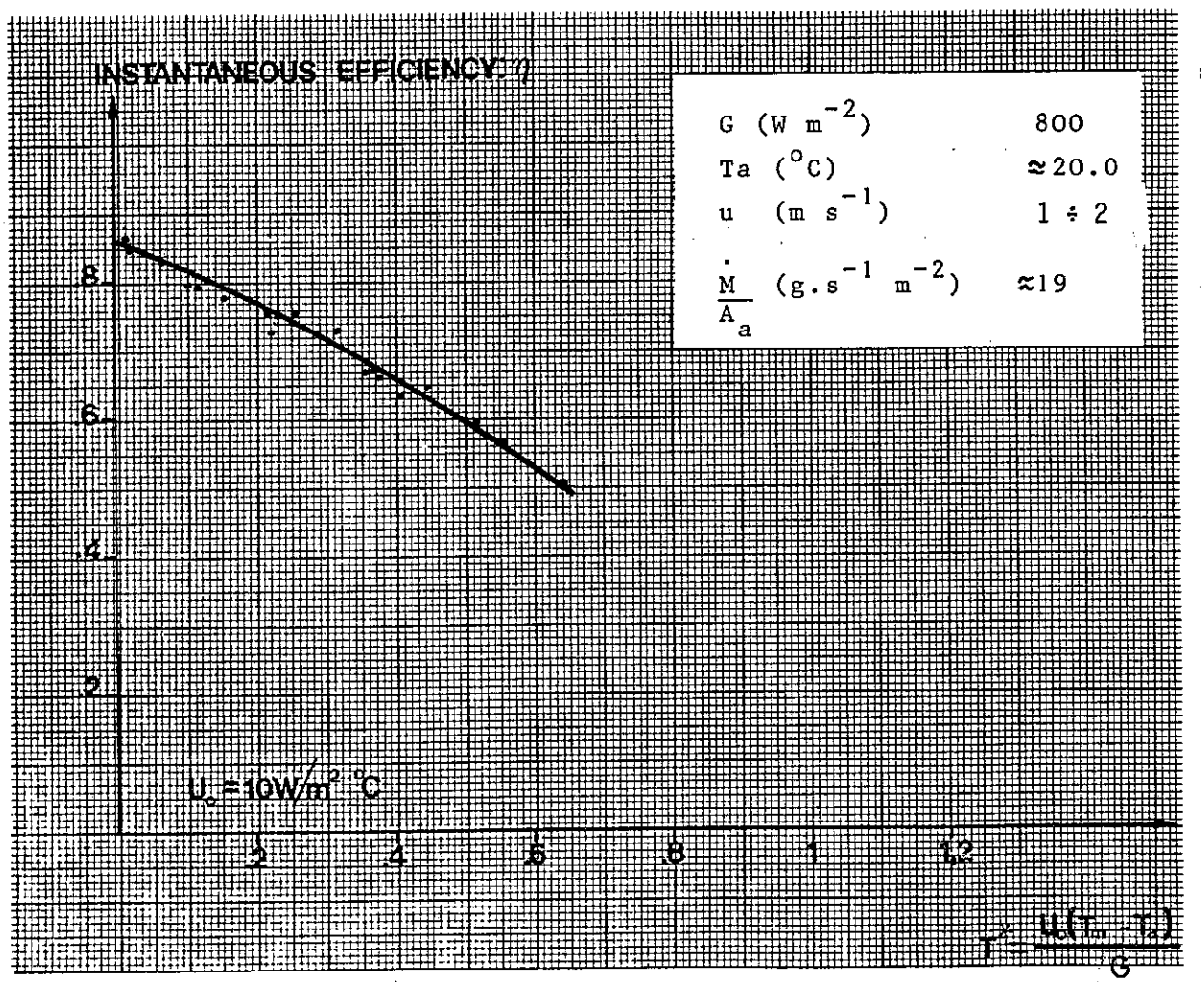

Fig. 26

RECOMMENDED EQUATION : $\eta = \eta_0 - a_1 T^* - a_2 (T^*)^2$

$\eta = 0.855 - 0.459 \cdot T^* - 0.105 \cdot (T^*)^2$

Instantaneous Efficiency Curve

THE INSTANTANEOUS EFFICIENCY η IS DEFINED BY : $\eta = \dfrac{\dot{Q}_u}{A_a \cdot G}$

q_u	: useful power extracted	☐	W
I	: incident radiation	☒	W/m^2
A	: reference area	☐	m^2

Specify which area is used for curve:
- ☐ gross area of collector
- ☒ aperture area
- ☐ absorber area

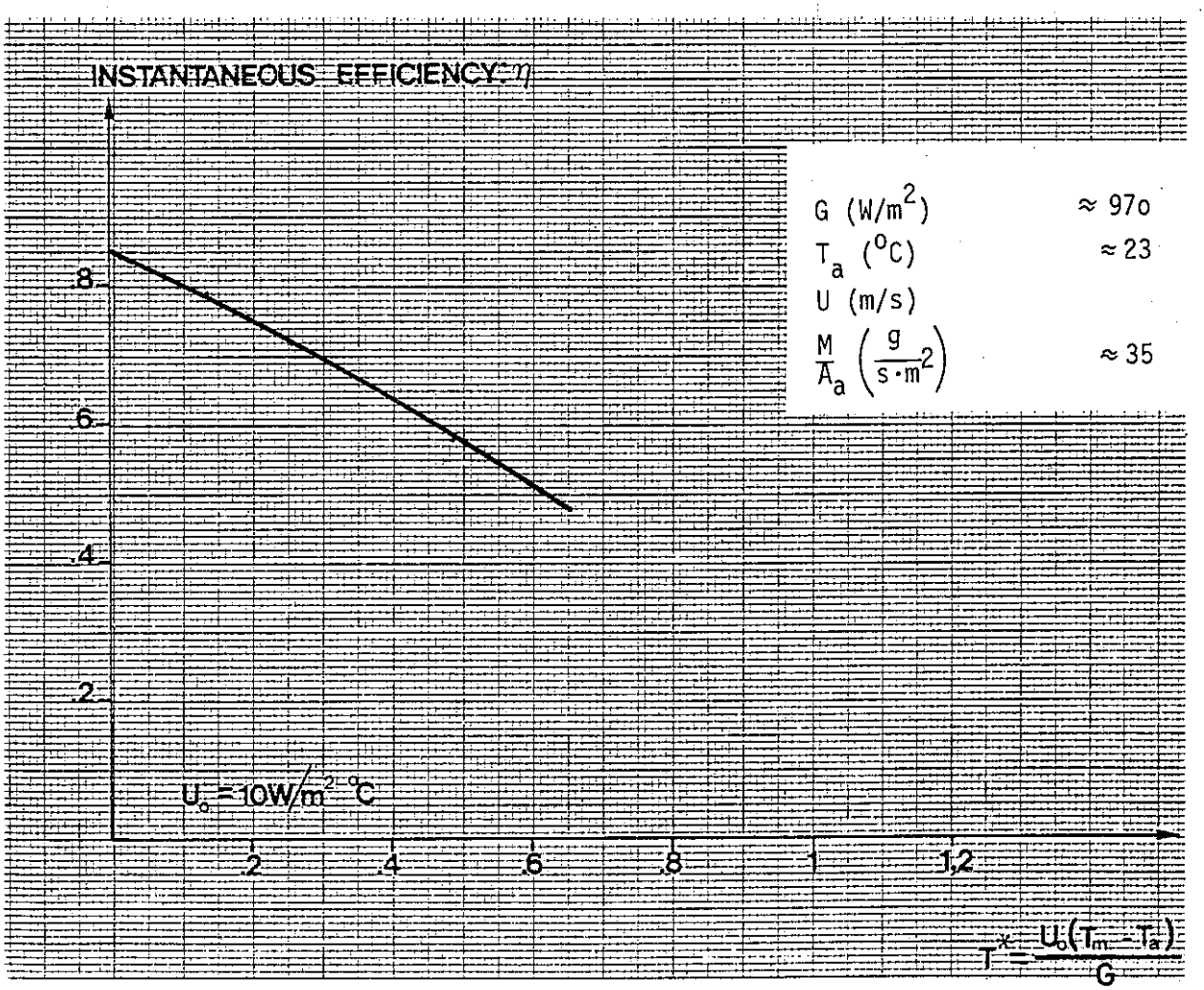

Fig. 27

RECOMMENDED EQUATION : $\eta = \eta_0 - a_1 T^* - a_2 (T^*)^2$

$\eta = 0.849 - 0.47 \cdot T^* - 0.156 \cdot (T^*)^2$

Test Institute: 4 Collector IEA-I

Instantaneous Efficiency Curve

THE INSTANTANEOUS EFFICIENCY η IS DEFINED BY: $\eta = \dfrac{\dot{Q}_u}{A_a \cdot G}$

$\dot{Q}_u$: useful power extracted	O	W
G : incident radiation	☒	W/m^2 ✗ 600 ⊡ 900 W/m^2
A : reference area	☒	m^2 1,0706

Specify which area is used for curve:

- O gross area of collector
- ☒ aperture area
- O absorber area

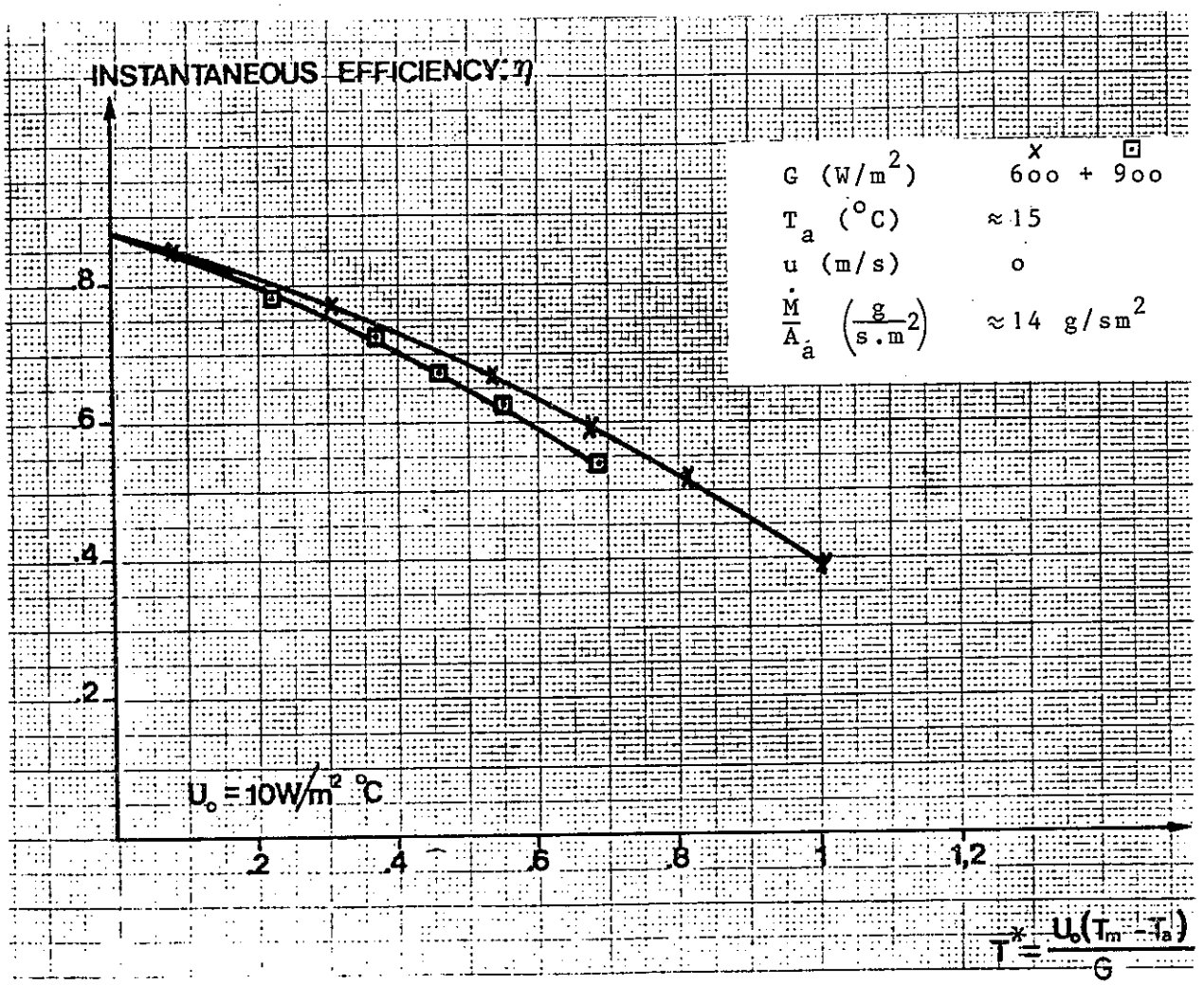

Fig. 28

RECOMMENDED EQUATION : $\eta = \eta_0 - a_1 T^* - a_2 (T^*)^2$

$\eta = 0{,}878 - 0{,}302 \cdot T^* - 0{,}166 \cdot (T^*)^2$ 600 W/m^2

$0{,}877 - 0{,}375 \cdot T^* - 0{,}143 \cdot (T^*)^2$ 900 W/m^2

Instantaneous Efficiency Curve

THE INSTANTANEOUS EFFICIENCY η IS DEFINED BY : $\eta = \dfrac{\dot{Q}_u}{A_a \cdot G}$

q_u : useful power extracted (W)

I : incident radiation (W/m^2)

A : reference area (m^2) $1.78\ m^2$

Specify reference area used for curve
- ☐ gross area of collector
- ☒ aperture area
- ☐ absorber area

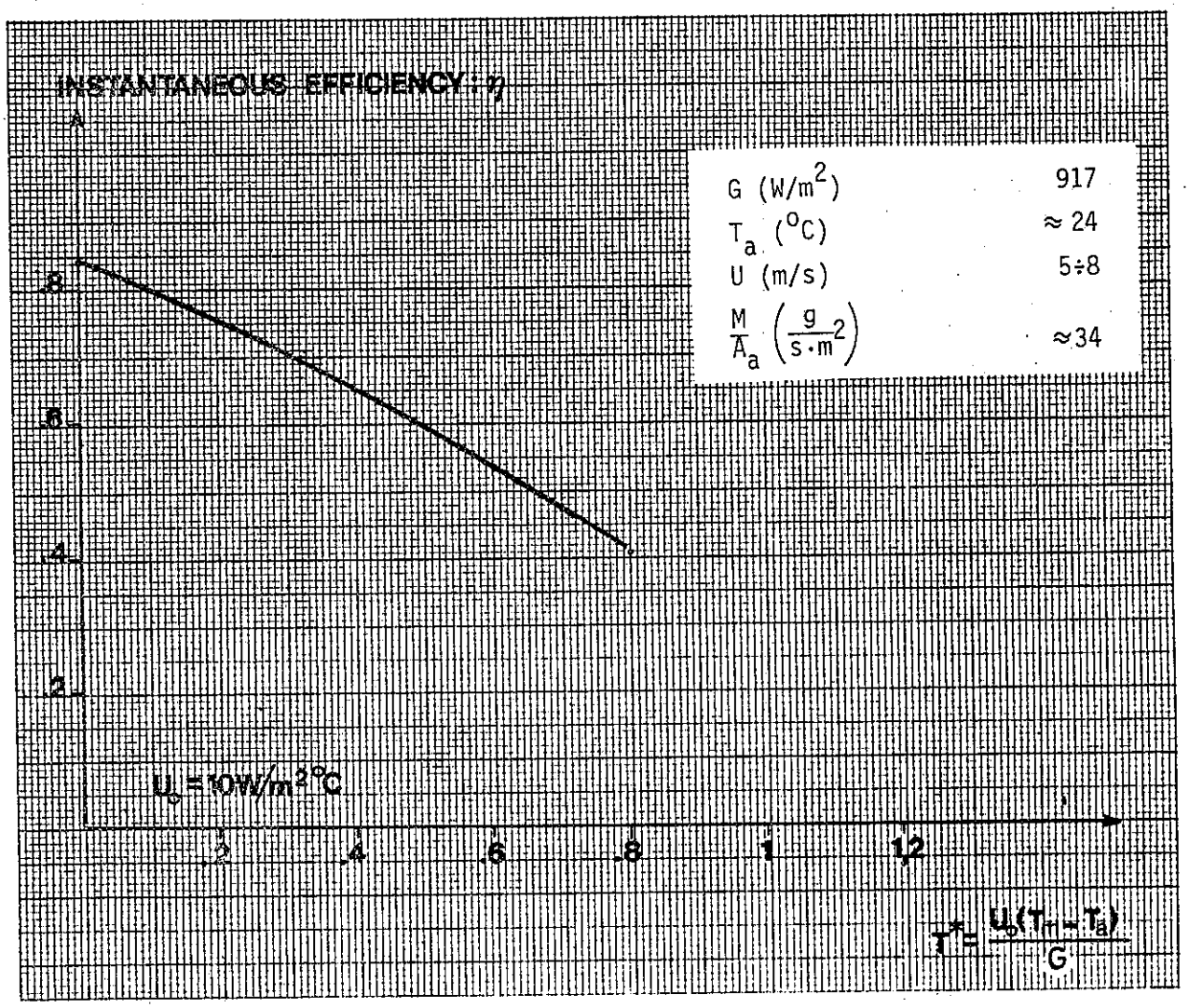

Fig. 29

RECOMMENDED EQUATION : $\eta = \eta_0 - a_1 T^* - a_2 (T^*)^2$

$$\eta = 0{,}840 - 0{,}411\ T^* - 0{,}161 (T^*)^2$$

Test Institute: 6 Collector IEA-I

Instantaneous Efficiency Curve

THE INSTANTANEOUS EFFICIENCY η IS DEFINED BY: $\eta = \frac{\dot{Q}_u}{A_a \cdot G}$

$\dot{Q}_u$: useful power extracted	O	W
G : incident radiation	O	W/m^2
A : reference area	☒	m^2 1.78

Specify which area is used for curve:

- O gross area of collector
- ☒ aperture area
- O absorber area

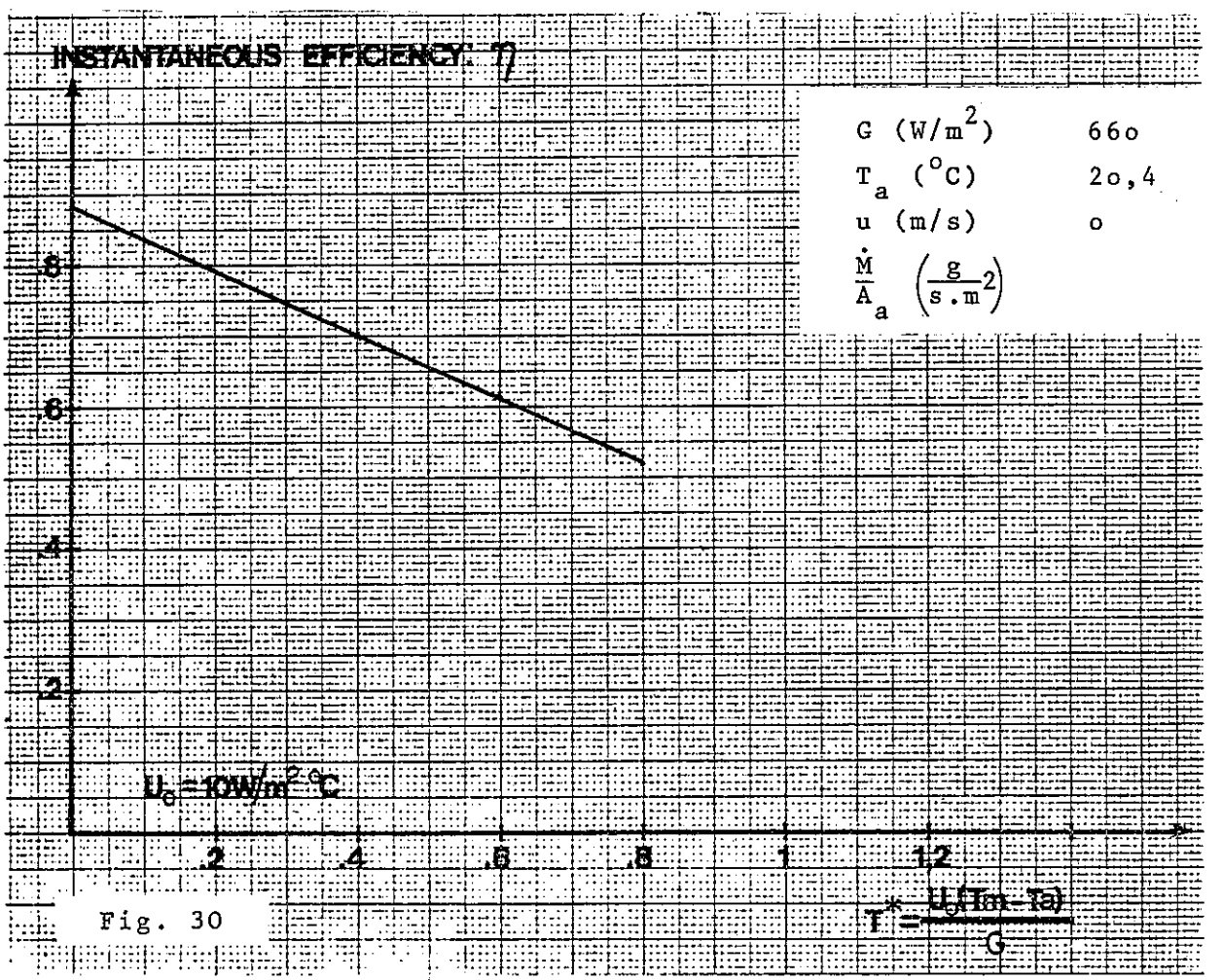

Fig. 30

RECOMMENDED EQUATION: $\eta = \eta_o - a_1 T^* - a_2 (T^*)^2$

$\eta = 0.874 - 5.044\ T^*$

PERFORMANCE COEFFICIENT : $\beta =$

Test Institute: 7 Collector IEA-I

Instantaneous Efficiency Curve

THE INSTANTANEOUS EFFICIENCY η IS DEFINED BY: $\eta = \dfrac{\dot{Q}_u}{A_a \cdot G}$

$\dot{Q}_u$: useful power extracted	0	W
G : incident radiation	X	W/m^2 1000
A : reference area	X	m^2 1,97 (A_g) or 1,79 (A_a)
Specify which area is used for curve:	X	gross area of collector
	X	aperture area
	0	absorber area

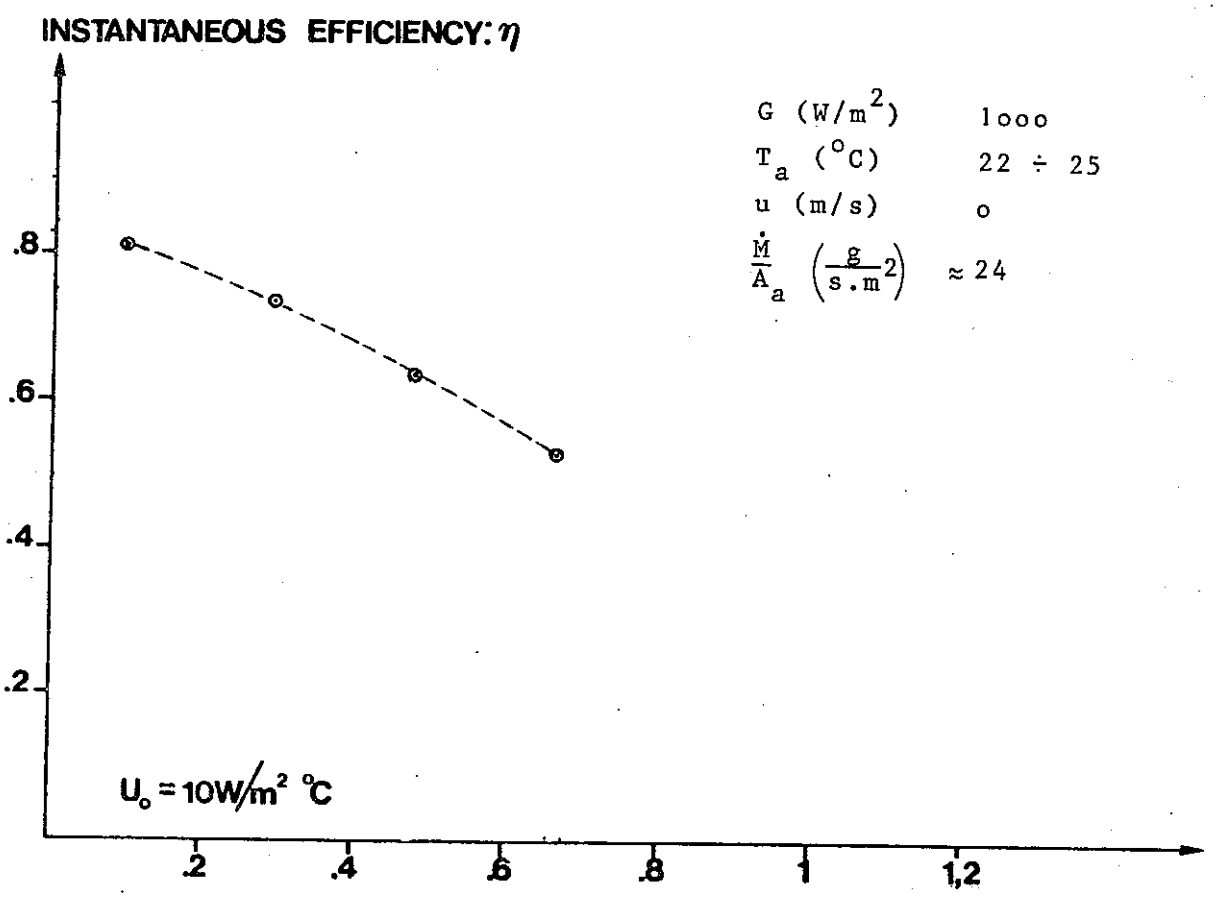

G (W/m^2)	1000
T_a (°C)	22 ÷ 25
u (m/s)	0
$\frac{\dot{M}}{A_a}$ $\left(\frac{g}{s \cdot m^2}\right)$	≈ 24

Fig. 31

RECOMMENDED EQUATION : $\eta = \eta_0 - a_1 T^* - a_2 (T^*)^2$

$\eta = 0.83 - 0.439\ T^*$

Test Institute: 1 Collector IEA-II

Instantaneous Efficiency Curve

THE INSTANTANEOUS EFFICIENCY η IS DEFINED BY: $\eta = \frac{\dot{Q}_u}{A_a \cdot G}$

$\dot{Q}_u$: useful power extracted — O W

G : incident radiation — O W/m^2

A : reference area — O m^2

Specify which area is used for curve:

- O gross area of collector
- X aperture area
- O absorber area

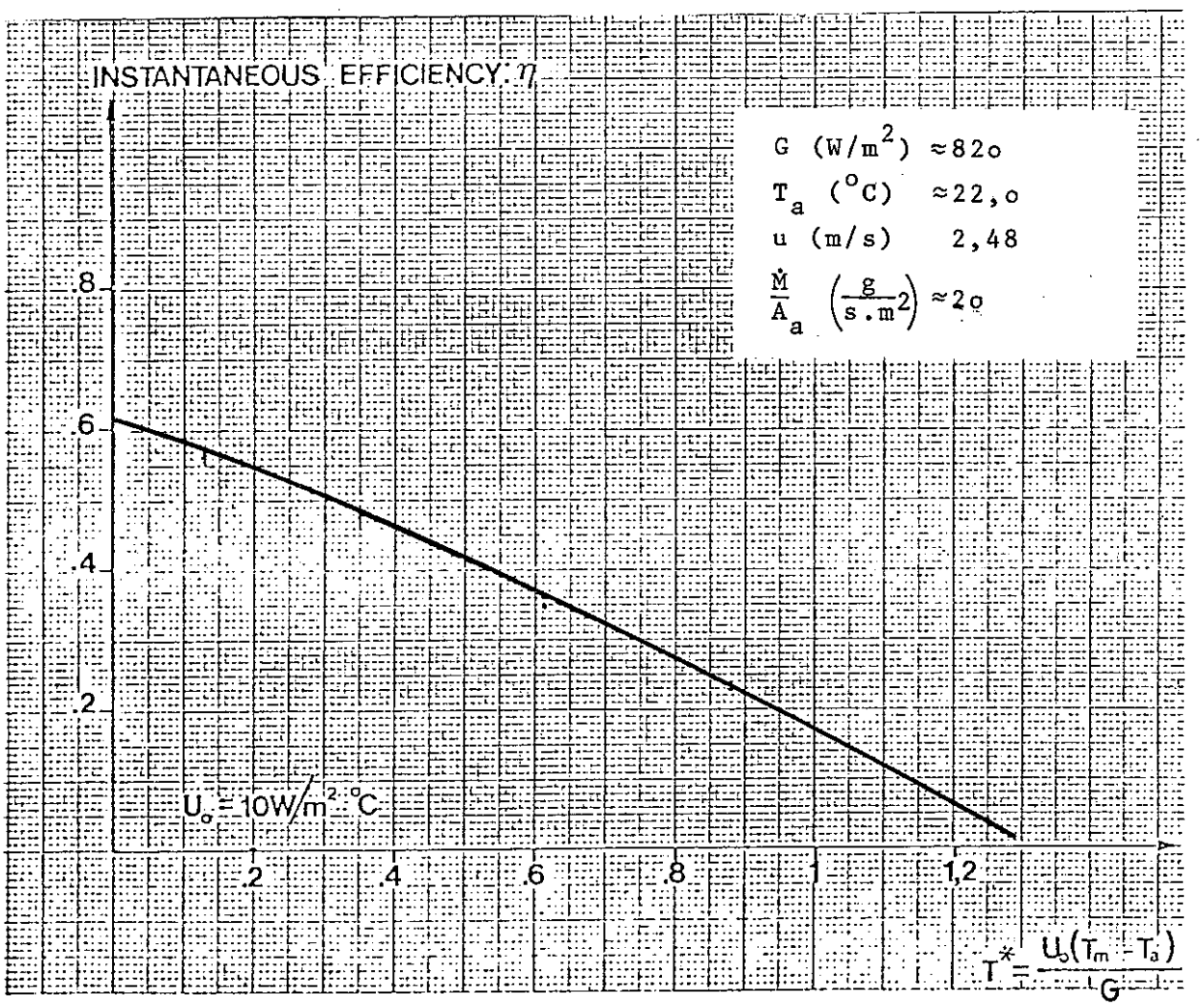

Fig. 32

RECOMMENDED EQUATION: $\eta = \eta_0 - a_1 T^* - a_2 (T^*)^2$

$\eta = 0.61_6 - 0.37_8 T^* - 0.063_7 T^{*2}$ (2nd order)
and
$0.62_7 - 0.44_2 T^*$ (linear)

Instantaneous Efficiency Curve

THE INSTANTANEOUS EFFICIENCY η IS DEFINED BY : $\eta = \dfrac{\dot{Q}_u}{A_a \cdot G}$

$\dot{Q}_u$	: useful power extracted	☐	W	
G	: incident radiation	☒	W/m²	750
A	: reference area	☒	m²	2.318

Specify which area is used for curve:
- ☐ gross area of collector
- ☒ aperture area
- ☐ absorber area

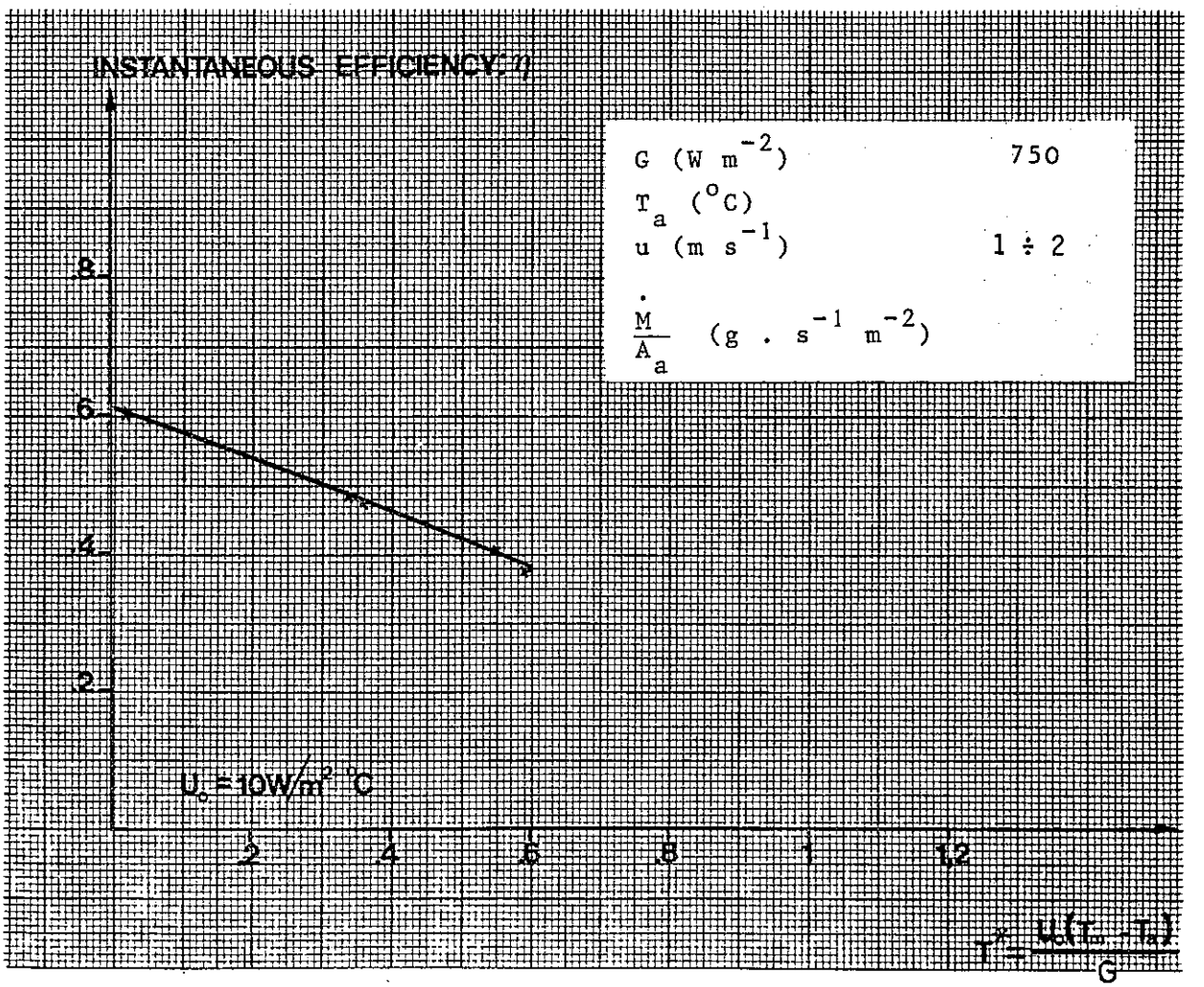

Fig. 33

RECOMMENDED EQUATION : $\eta = \eta_0 - a_1 T^* - a_2 (T^*)^2$

$\eta = 0.610 - 0.349\ T^* - 0.057\ (T^*)^2$

Instantaneous Efficiency Curve

THE INSTANTANEOUS EFFICIENCY η IS DEFINED BY : $\eta = \dfrac{\dot{Q}_u}{A_a \cdot G}$

$\dot{Q}_u$	: useful power extracted	☐	W
G	: incident radiation	☒	W/m^2 1000
A	: reference area	☐	m^2

Specify which area is used for curve:
- ☐ gross area of collector
- ☐ aperture area
- ☐ absorber area

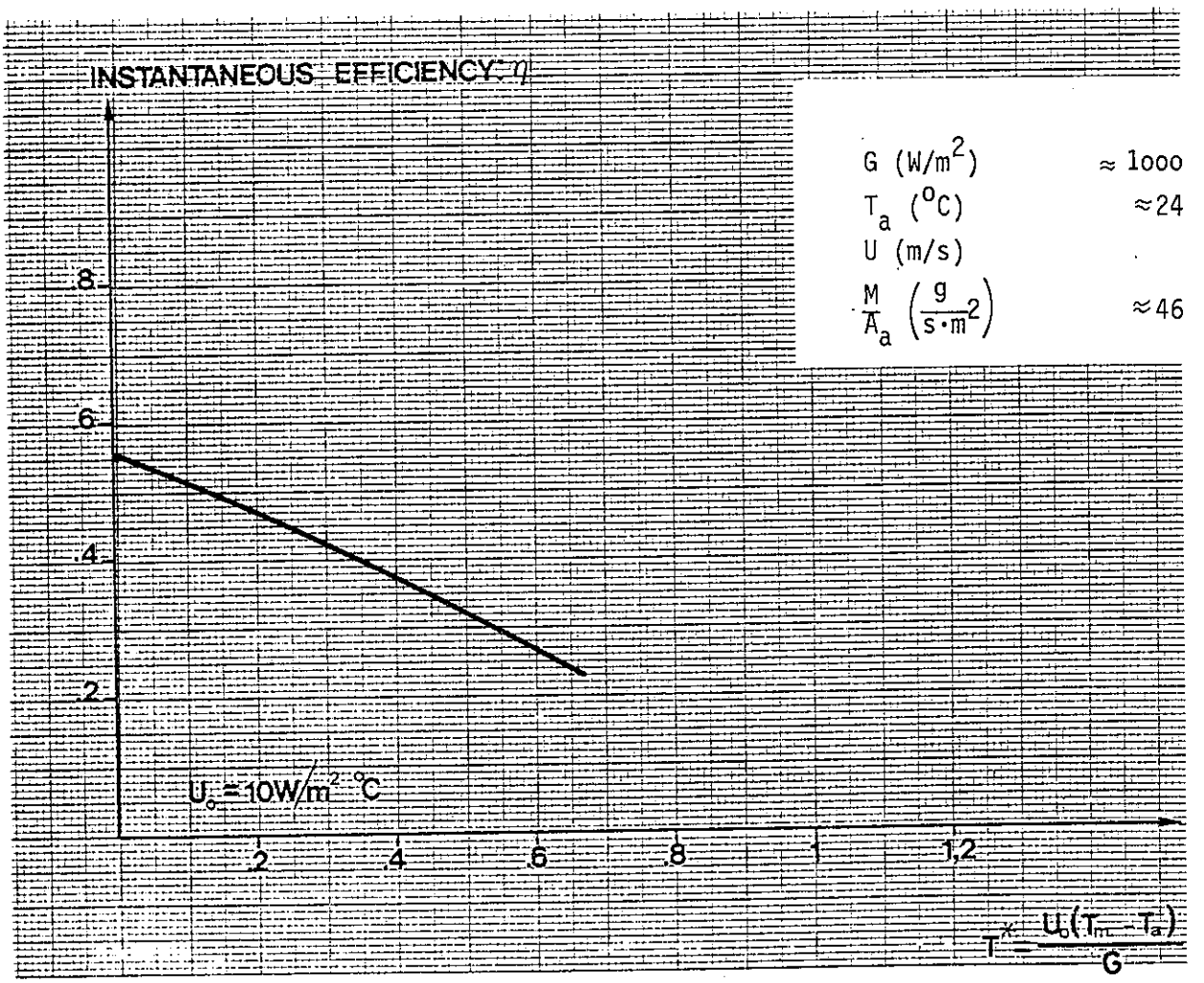

Fig. 34

RECOMMENDED EQUATION : $\eta = \eta_0 - a_1 T^* - a_2 (T^*)^2$

$\eta = 0.555 - 0.391 \cdot T^* - 0.155 \cdot (T^*)^2$

Test Institute: 4 Collector IEA-II

Instantaneous Efficiency Curve

THE INSTANTANEOUS EFFICIENCY η IS DEFINED BY: $\eta = \dfrac{\dot{Q}_u}{A_a \cdot G}$

$\dot{Q}_u$: useful power extracted	o	W
G : incident radiation	o	W/m^2 x 6oo ⊡ 9oo W/m^2
A : reference area	☒	m^2 1.o46

Specify which area is used for curve:

- o gross area of collector
- ☒ aperture area
- o absorber area

INSTANTANEOUS EFFICIENCY : η

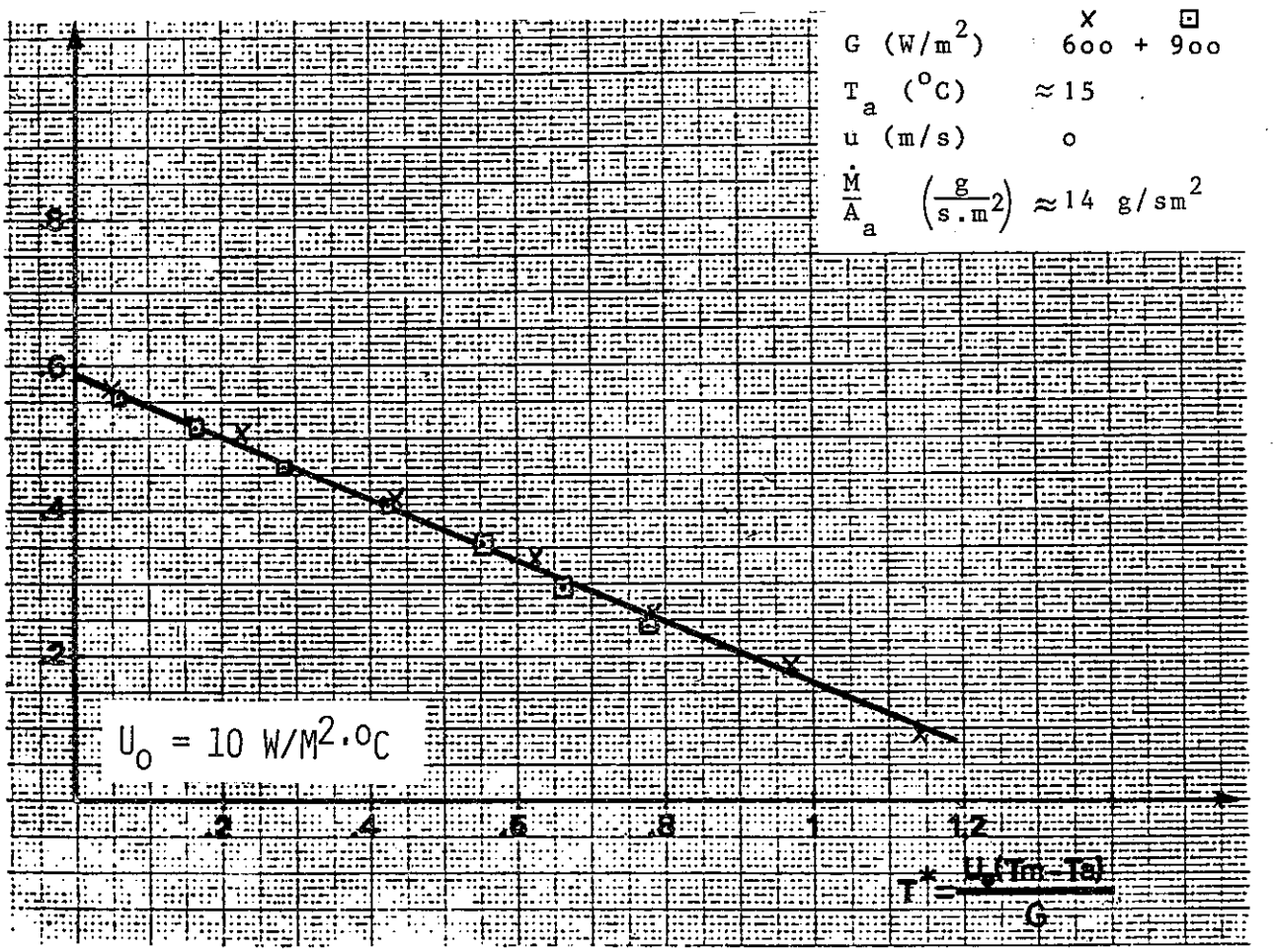

Fig. 35

RECOMMENDED EQUATION : $\eta = \eta_0 - a_1 T^* - a_2 (T^*)^2$

$\eta = 0{,}5829 - 0{,}3904 \cdot T^* - 0{,}0295 (T^*)^2$

Test Institute: 7 Collector IEA-II

Instantaneous Efficiency Curve

THE INSTANTANEOUS EFFICIENCY η IS DEFINED BY: $\eta = \frac{\dot{Q}_u}{A_a \cdot G}$

$\dot{Q}_u$: useful power extracted	O	W	
G : incident radiation	O	W/m^2	1ooo
A : reference area	☒	m^2	2.49 (A_g) or 2.30 (A_a)

Specify which area is used for curve:

- ☒ gross area of collector
- ☒ aperture area
- O absorber area

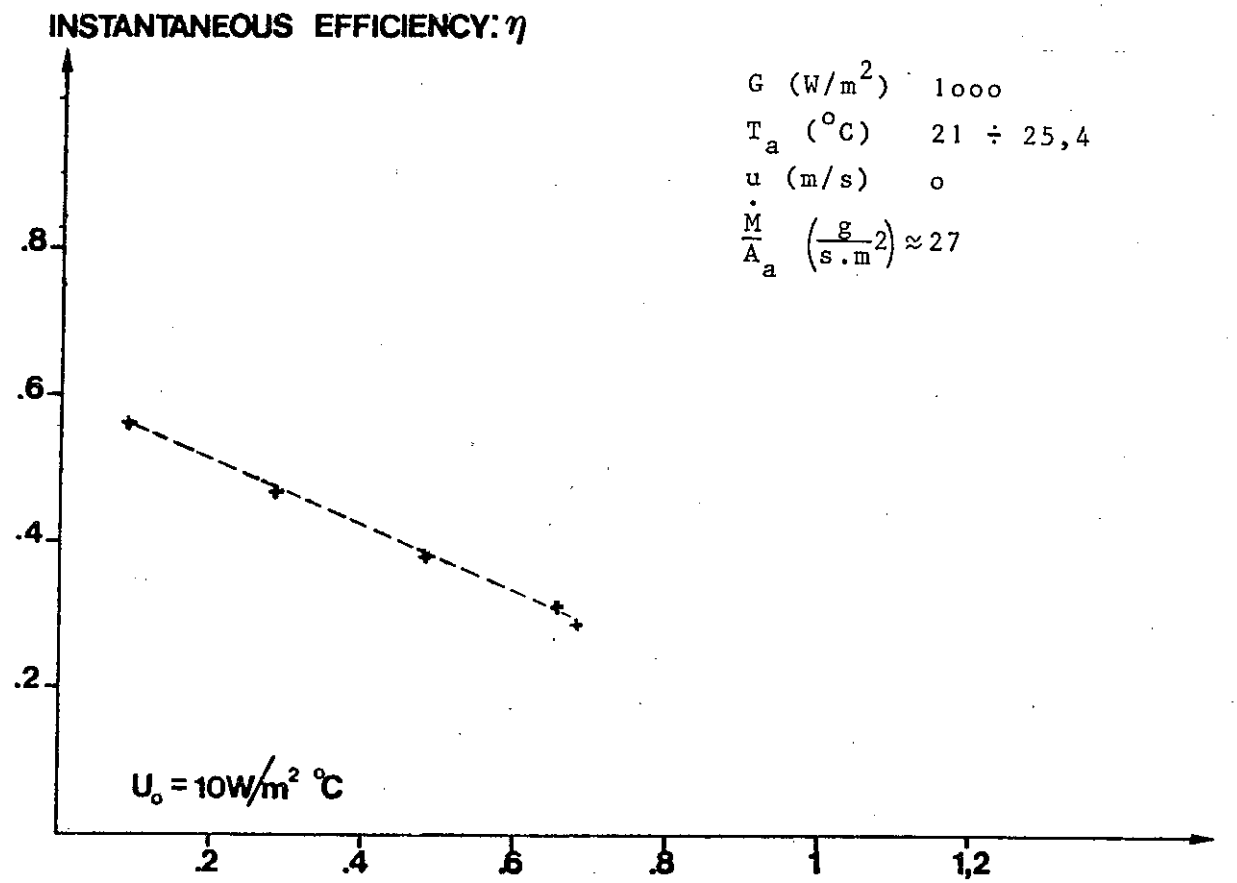

Fig. 36

RECOMMENDED EQUATION: $\eta = \eta_0 - a_1 T^* - a_2 (T^*)^2$

$\eta = 0.6067 - 0.390\ T^* - 0.0295\ (T^*)^2$

APPENDIX 1

ASHRAE-Specification 93 - 77

METHODS OF TESTING TO DETERMINE THE THERMAL PERFORMANCE OF SOLAR COLLECTORS

7.3 INDOOR TESTING WITH A SOLAR SIMULATOR

A solar simulator may be used in lieu of outdoor testing to determine the steady state thermal performance of the solar collector under controlled conditions of wind and ambient temperature. References [15], [16] ,[5] describe typical simulators used for testing collectors. Solar simulators employed in the testing procedure shall have the following characteristics.

7.3.1 SPECTRAL QUALITIES

The simulator shall duplicate the spectrum of average North American sunlight as closely as possible. This average is best represented by an air-mass 2 solar spectrum [15]. The measured energy spectrum shall not deviate from the air-mass 2 spectrum more than specified in the following table.

Band λ µm	Air Mass 2, Percent of Energy in Band	Maximum Deviation of Simulator
0.3 - 0.4	2.7	15.%
0.4 - 0.7	44.4	9
0.7 - 1.0	28.6	3
1.0	24.3	10

In addition, the calculated solar absorptivity, α , of the spectrally selective surface described in Reference [14] irradiated by the simulator shall not differ more than 1 percent from the value measured under air-mass 2 sunlight.

There shall not be a significant change in the simulator's energy spectrum for variations in power output. The calculated solar absorptivity of the above specified selective surface [18] irradiated by the simulator shall not change by more than 1 % for a change in radiation flux from 0.45 to 0.75 of one Solar Constant.

7.3.2 UNIFORMITY

The departure from uniformity of the illumination of the solar simulator beam over the test plane (the plane of the collector aperture) shall be such that the high and low irradiation values of the illuminated plane shall not exceed $\pm$ 10 % of the average illumination.

7.3.3 COLLIMATION

The collimation shall be such that 95 % of the energy output of the simulator is within a subtended angle of less than 12 degrees. A collimation of greater than this is required for collectors with concentration ratios greater than 2/1.

7.3.4 AIR FLOW ACROSS THE COLLECTOR

A fan shall be provided to cause a substantially uniform air flow across the collector surface. The fan shall be capable of producing an air velocity of at least 3.5 m/sec (7.6 mph).

7.3.5 SIMULATOR - COLLECTOR CONFIGURATION FACTOR

The collector configuration factor between the solar simulator surface and the solar collector shall not exceed 0.05.

APPENDIX 2

AFNOR-Norm P 50 - 501

AFNOR 77511

CAPTEURS SOLAIRES MESURE DES PERFORMANCES THERMIQUES

Éditée par L'ASSOCIATION FRANÇAISE DE NORMALISATION (AFNOR) — Tour EUROPE CEDEX 7 92080 PARIS LA DÉFENSE — Tél (1) 788-11-11

NORME EXPÉRIMENTALE	CAPTEURS SOLAIRES MESURE DES PERFORMANCES THERMIQUES	P 50-501 Décembre 1977

1 GÉNÉRALITÉS

1.1 OBJET

La présente norme expérimentale a pour objet de définir des méthodes d'essais destinées à mesurer les performances thermiques des capteurs solaires utilisés pour le chauffage d'un fluide.

1.2 DOMAINE D'APPLICATION

La présente norme s'applique aux capteurs solaires utilisant un liquide comme fluide caloporteur et ne comportant qu'une entrée et une sortie.

Le capteur peut être un capteur à concentration pourvu que le plan d'ouverture de l'appareil puisse être déterminé.

Elle ne s'applique pas aux capteurs dans lesquels le dispositif de stockage thermique fait partie intégrante du capteur et dans lesquels les opérations de captage et de stockage de l'énergie ne peuvent être séparées en vue d'effectuer les mesures nécessaires, ni aux capteurs dans lesquels intervient un changement de phase au cours du processus de captage de l'énergie.

1.3 NOTATIONS ET DÉFINITIONS

— Voir annexes A 1 et A 2.

2 MESURE DE PERFORMANCES THERMIQUES

2.1 PRINCIPE DES MESURES

Les performances thermiques sont déterminées par la mesure des puissances extraites du capteur, le débit massique de fluide caloporteur et la différence entre la température d'entrée et la température ambiante étant maintenus constants.

Ces mesures sont effectuées soit en ensoleillement naturel soit en chambre climatique.

Les observations relatives à la présente norme expérimentale doivent être adressées à l'AFNOR, Tour Europe, CEDEX 7 92080 PARIS LA DÉFENSE

Afnor 77511 P 50-501 1er Tirage 77-12

Solar captors. Measurement of thermal performances

Sonnenenergiespeicher — Messung der Wärmeleistung

2.2 APPAREILLAGE

2.2.1 Mesure des rayonnements

Mesurer l'éclairement énergétique du rayonnement global d'un pyranomètre de classe 2 au moins (*) étalonné depuis moins de deux ans par le laboratoire effectuant l'étalonnage suivant les règles de l'O.M.M. (Organisation Météorologique Mondiale).

Mesurer l'éclairement énergétique du rayonnement total au moyen d'un pyrradiomètre étalonné depuis moins d'un an.

2.2.2 Mesure des températures

Utiliser un appareillage tel que :

— l'incertitude sur la mesure de la différence de température du fluide caloporteur entre l'entrée et la sortie soit inférieure ou égale à la plus grande des deux valeurs suivants 2 % ou 0,1 °C.

— l'incertitude sur la mesure de la température de l'air ambiant et de la température du fluide caloporteur à l'entrée du capteur soit inférieure ou égale à 0,5 °C

2.2.3 Mesure du débit massique du fluide caloporteur

Utiliser un appareillage tel que l'incertitude de la mesure soit inférieure à 1 %.

2.3 DISPOSITIONS GÉNÉRALES

2.3.1 Essayer les capteurs dans l'état où ils sont livrés au laboratoire par le constructeur, sans vieillissement préalable.

2.3.2 Lorsque le fluide caloporteur est de l'eau, prendre un débit massique normal de 30 kilogrammes par heure et par mètre carré de capteur à 2 % près. (Soit 8,33 x 10^{-3} kg/s.m²). Dans le cas de fluides caloporteurs différents, prendre l'équivalent en eau.

Utiliser un dispositif d'essai tel que les variations de débit massique au cours d'un essai soient inférieures à 1 %.

2.3.3 Monter les pyranomètres et les pyrradiomètres dans le plan d'ouverture du capteur, à mi hauteur et à moins de 0,50 m du bord de celui-ci de façon à ce qu'aucune énergie appréciable ne soit réfléchie sur ces appareils (**).

2.3.4 Placer les sondes de mesure de températures d'entrée et de sortie du caloporteur à moins de 0,15 m de l'entrée et de la sortie et conformément aux règles de l'art.

2.3.5 Les écarts (T_e — T_a) entre la température d'entrée du fluide caloporteur et la température de l'air ambiant doivent être égaux à 2 °C près aux valeurs fixées pour les essais. (voir2.6).

2.4 DISPOSITIONS PARTICULIÈRES POUR LES MESURES EN ENSOLEILLEMENT NATUREL

2.4.1 Montage du dispositif d'essai

2.4.1.1 Choisir un site tel que la hauteur angulaire de tout obstacle situé dans le demi-espace en avant du capteur ne soit pas supérieur à 15° au-dessus du plan horizontal passant par la base du capteur.

(*) *Voir annexe 2 pour le classement des pyranomètres.*

(**) *Le pyrradiomètre est destiné à obtenir la proportion de rayonnement de grande longueur d'onde ($\lambda > 3\ \mu m$) dans le rayonnement reçu par le capteur ; la valeur acceptable de cette proportion sera précisée ultérieurement.*

2.4.1.2 Placer le dispositif d'essai de telle sorte

— que le capteur ne reçoive aucune énergie appréciable réfléchie par des bâtiments ou toute autre surface avoisinante. Disposer, si nécessaire, un écran destiné à protéger le capteur.

— qu'aucune ombre ne puisse être projetée sur le capteur au cours des essais. (Par exemple antenne, poteau électrique etc.).

2.4.1.3 Monter le capteur sur un support rigide incliné à 45° par rapport à l'horizontale, sauf spécifications particulières du constructeur.

Réaliser le montage de façon à n'apporter aucune perturbation dans le bilan thermique du capteur. Orienter le capteur de telle sorte que l'angle d'incidence par rapport à la normale du plan d'ouverture soit inférieur à 40° pendant toute la durée des essais.

2.4.1.4 Placer la sonde de température ambiante sous un abri protecteur du rayonnement, bien ventilé, le bas étant à mi-hauteur du capteur et à moins de 0,50 m de celui-ci.

2.4.2 Conditions d'essai

Avant d'effectuer toute mesure faire fonctionner à température d'entrée et débit établis, pendant une période d'au moins 1 heure au cours de laquelle les conditions météorologiques auront été sensiblement stables.

2.4.2.1 Effectuer l'essai par énergie incidente globalement décroissante. Pendant l'heure de fonctionnement préalable, enregistrer la courbe d'éclairement énergétique fourni par le pyranomètre. Tracer autrour de cette courbe deux droites parallèles passant respectivement par les points B et C de même abcisse que le point A pris comme point d'essai sur la courbe d'éclairement énergétique et d'ordonnées égales à E_{ng} (A) + 5 % et E_{ng} (A) — 5 %. (Voir figure 1).

L'essai n'est considéré comme valable que s'il est possible d'inscrire la totalité de la courbe entre ces deux droites dont la pente négative doit avoir une valeur absolue inférieure ou égale à 120 W/m².h. Toutefois, les débordements de durée inférieure à 5 s sont admis.

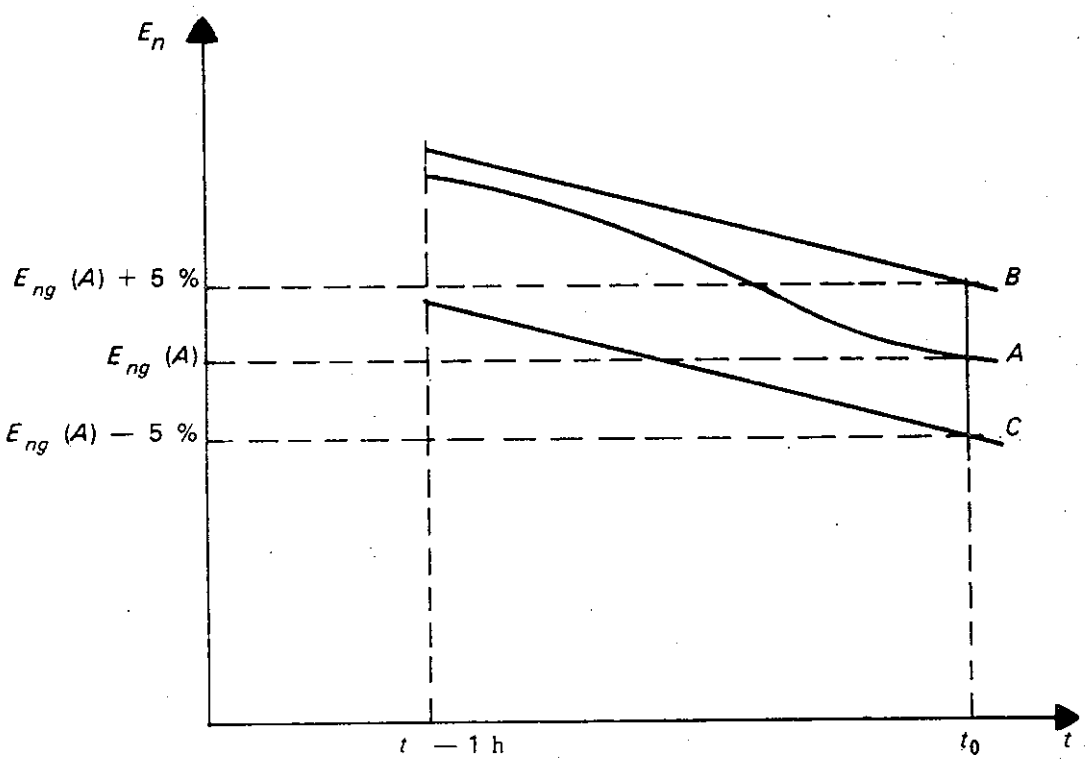

Figure 1 — Exemple de courbe d'éclairement énergétique

2.4.2.2 La température de l'air ambiant doit être comprise entre 5 °C et 30 °C.

2.4.2.3 Mesurer la vitesse de l'écoulement de l'air sur le site à 1 m au-dessus du capteur à 15 % près, le seuil de démarrage de l'appareil étant inférieur à 1 m/s.

Retenir les moyennes calculées sur des périodes de dix minutes précédant les points de mesure.

Les valeurs de ces moyennes doivent être comprises entre 1,6 m/s et 5,4 m/s.

Noter l'orientation moyenne de l'écoulement de l'air et l'orientation moyenne du capteur.

2.4.2.4 Procéder à une mesure indicative des proportions de l'éclairement énergétique provenant de l'ensoleillement direct et diffus en utilisant le même pyranomètre ou un autre de même type placé dans les mêmes conditions.

2.5 DISPOSITIONS PARTICULIÈRES POUR LES MESURES EN CHAMBRE CLIMATIQUE

2.5.1 Dispositif d'essai

Mesurer l'éclairement énergétique au moyen du pyranomètre en le montant à l'endroit où sera placé le capteur, dans le plan où se situera le plan d'ouverture de celui-ci.

Effectuer les mesures aux nœuds d'un réseau à mailles carrées de pas maximal 0,25 m.

Retenir comme valeur de l'éclairement énergétique la moyenne arithmétique des mesures faites aux nœuds d'un réseau à mailles carrées de pas maximal 0,25 m.

Aucune valeur mesurée ne doit s'écarter de plus de 10 % de cette moyenne.

De plus la valeur moyenne ne doit pas varier de plus de 5 % pendant la durée d'un essai.

Le vérifier au moyen d'un pyranomètre et d'un pyrradiomètre placés dans une zone où l'éclairement est au moins égale à 80 % de l'éclairement maximal.

Placer derrière le capteur, à une distance comprise entre 5 cm et 25 cm de celui-ci, au moins une sonde par mètre carré pour la mesure de la température ambiante. Retenir comme valeur de calcul la moyenne arithmétique des températures mesurées.

2.5.2 Conditions d'essai

La température de l'air ambiant doit être comprise entre 15 °C et 20 °C et rester constante à 0,5 °C près pendant la durée de l'essai.

La température d'entrée du fluide caloporteur doit être constante à 0,5 °C près.

Faire les mesures si, après avoir laissé stabiliser la différence de température entrée/sortie du fluide caloporteur pendant une période de dix minutes, la variation de cette différence de température est inférieure à 0,1 °C.

Placer les faces avant et arrière du capteur dans une veine d'air horizontale et parallèle au plan de la couverture du capteur de vitesse égale à 2 m/s ± 0,5 m/s sur l'ensemble de la surface. Maintenir ces conditions pendant toute la durée de l'essai.

2.6 TECHNIQUE DES ESSAIS

2.6.1 Essais de base

Ces essais sont effectués sur chaque type (*) de capteur dans chacune des dimensions sauf décision motivée du laboratoire.

Les valeurs des paramètres pour chacun des essais sont données dans le tableau 1.

(*) *On entend par type de capteur un capteur d'une conception donnée mais pouvant être fabriqué avec des dimensions différentes.*

TABLEAU 1

Numéro de l'essai	Éclairement énergétique E_{ng} W m²	Angle d'incidence degré		Écart entre la température d'entrée du fluide et la température ambiante $T_e - T_a$ °C	Débit massique du fluide m kg/s
		En chambre climatique	En ensoleillement naturel		
1	800	0	entre	0 °C	m_n (*)
2	800	0	0 et 40	20 °C	m_n
3	800	0	"	40 °C	m_n
4	800	0	"	60 °C	m_n
5	800	0	"	40 °C	$1/2\, m_n$
(*) m_n : *débit normal.*					

2.6.2 Essais complémentaires

Ces essais peuvent n'être effectués que sur un capteur par type.

Essai n° 6 : Influence de l'intensité de l'éclairement énergétique

Placer le capteur en chambre climatique dans les conditions suivantes :

- Éclairement énergétique 400 ± 20 W/m².
- Angle d'incidence 0°.
- Écart entre la température d'entrée du fluide et la température ambiante : 20 °C.

Essai n° 7 : Influence combinée de l'intensité de l'éclairement énergétique et de l'angle d'incidence du rayonnement direct.

Placer le capteur en ensoleillement naturel dans les conditions suivantes :

- Éclairement énergétique 400 ± 20 W/m².
- Angle d'incidence supérieur à 50°.
- $T_e - T_a = 20$ °C.

Essai n° 8 : Détermination de la température maximale du capteur sous un éclairement énergétique donné.

Placer le capteur en chambre climatique dans les conditions suivantes :

- Éclairement énergétique : 400 W/m².
- Angle d'incidence 0°.

Relier l'entrée et la sortie du capteur.

Faire circuler le fluide caloporteur au débit normal. Soumettre le capteur à l'éclairement énergétique jusqu'à obtention de la température d'équilibre. Cette température d'équilibre est considérée comme étant atteinte lorsque $T_s - T_e \leqslant 0{,}5$ °C.

Retenir la valeur atteinte après stabilisation c'est-à-dire lorsque la variation de cette valeur est inférieure à 0,5 °C en 10 minutes.

Essai n° 9 et 10 : Mesures des pertes arrières et latérales

Ces essais peuvent se dérouler en chambre climatique ou en ensoleillement naturel, les conditions de situation, d'inclinaison, de température ambiante, d'écoulement d'air étant les mêmes que celles des essais de base.

Recouvrir entièrement la face d'entrée du capteur d'un isolant réfléchissant le rayonnement sur ses deux faces et du coefficient de transmission thermique $K' = 0{,}5$ W/m².°C.

Faire circuler le fluide caloporteur au débit normal (dans le cas de capteurs dissymétrique, appliquer une procédure spécifique).

Procéder à 2 mesures, pour les écarts entre la température d'entrée du fluide et la température ambiante ($T_e - T_a$) égaux à 40 °C et 60 °C.

Vérifier que le capteur ne reçoit aucune énergie par rayonnement en s'assurant que la différence entre la température de l'air ambiant et la température des parois et du fond du capteur est inférieure à 1 °C.

Indiquer les pertes, après stabilisation de la température de sortie.

Essai n° 11 : Mesure de l'inertie du capteur

Effectuer cet essai en chambre climatique. Couvrir le capteur par un écran réfléchissant. Faire circuler le fluide caloporteur au débit normal, sa température d'entrée étant égale à la température ambiante.

Appliquer un éclairement énergétique de 800 W/m². Retirer rapidement l'écran.

Enregistrer la variation de la température de sortie du liquide caloporteur T_s en fonction du temps.

Noter sa valeur d'équilibre T_q (cette valeur est considérée comme atteinte lorsque sa variation est inférieure à 0,5 °C en 10 minutes).

Noter le temps nécessaire à partir de l'instant où l'écran a été retiré, pour que la température de sortie du fluide T_s soit telle que $(T_s - T_a) = 0{,}9\ (T_q - T_a)$.

où :

T_q = température de sortie du fluide caloporteur, lorsque le capteur a atteint un régime d'équilibre.

CONDITIONS DES ESSAIS
(TABLEAU RÉCAPITULATIF)

Grandeur	Incertitude de la mesure	Variations tolérées autour de la position d'équilibre		Différence tolérée avec la valeur nominale	
		naturel	artificiel	naturel	artificiel
Température ambiante T_a	± 0,5 °C	5 °C < T_a < 30 °C	± 0,5 °C	5 °C < T_a < 30 °C	15 °C < T_a < 20 °C
Température d'entrée d'eau T_e	± 0,5 °C		± 0,5 °C		± 0,5 °C
$T_e - T_a$			± 1 °C	± 2 °C	± 2 °C
$T_s - T_e$	± 2 %		± 0,1 °C		
Débit caloporteur	± 1 %	± 1 %	± 1 %	± 2 %	± 2 %
E_{ng}	Classe ⩽ 2	Pente moyenne ⩽ 120 W/m².h ± 5 % Voir 2.4.1	± 10 % dans l'espace ± 5 % dans le temps	± 5 %	± 5 %
Vitesse de l'écoulement d'air	± 15 % ± seuil de démarrage 1 m/s	1,6 < v < 5,4 m/s	± 0,5 m/s	1,6 < v < 5,4 m/s	

2.7 EXPRESSION DES RÉSULTATS

Pour chacun des essais de base définis à l'article 2.6.1.

Calculer la puissance thermique utile du capteur.

$$Q = m \times C_p \times (T_s - T_e)$$

— calculer la puissance solaire $A \times E_{ng}$

A = superficie du capteur.

— calculer le rendement hors-tout du capteur

$$\eta = \frac{Q}{A \times E_{ng}}$$

— à titre indicatif calculer éventuellement, quand c'est techniquement possible, le rendement par rapport à la superficie d'entrée du capteur : Aa.

2.8 PROCÈS-VERBAL D'ESSAI

Le procès-verbal d'essai devra comporter :

— un tableau de résultats conforme au modèle ci-après.

— la valeur indicative de la perte de charge du capteur pour le débit normal,

— les motifs éventuels ayant conduit le laboratoire à ne pas effectuer certains des essais de base,

Le procès-verbal d'essai sera accompagné d'une fiche conforme au modèle ci-après comportant les renseignements fournis par le constructeur. Le laboratoire vérifiera les dimensions données par celui-ci.

TABLEAU DE PRÉSENTATION DES RÉSULTATS (Grandeurs mesurées)

Capteur :

Marque et référence :

Superficies A = A_a =

Laboratoire :

Date de l'essai :

Éclairement : en ensoleillement naturel/en chambre climatique.

N° ESSAI	E_{ng} pyranomètre (W m²)	E_{nt} pyrradiomètre (W m²h)	Éclairement énergétique solaire diffus % E_{ng}	$\frac{\Delta E_{ng}}{\Delta t}$ (W m²)	$T_e - T_a$ (°C)	$T_s - T_e$ (°C)	T_a (°C)	Débit massique (kg S)	Vitesse moyenne d'écoulement d'air	Puissance thermique utile Q	Rendement hors-tout $\frac{Q}{A \times E_{ng}}$
1 2 3 4 5											
6											
7											
8					Température d'équilibre °C						
9 10						$T_e - T_s$					Pertes (W)
11					Température d'équilibre T_q °C						Temps de montée

FICHE DE RENSEIGNEMENTS

Fabricant : (nom, adresse) : .....

Dénomination commerciale du capteur ou référence : .....

Dimensions hors tout : x x cm

Poids à vide : ..... Rempli d'eau : .....

Absorbeur — nature du matériau : .....
nature du revêtement absorbant : .....

Couverture — nature du matériau : .....
nombre : .....

Coffre — nature du matériau et de son/ses revêtements : .....

Isolant — nature(s) : .....
épaisseur(s) : .....

Joints — nature des différents joints : .....

Système d'ouverture du capteur — description : .....

Pression maximale de service : ..... kPa

Température limite d'utilisation : ..... degrés Celcius

Perte de charge pour le débit normal : ..... Pa

Fluides caloporteurs pouvant être employés : .....

Remarques que le constructeur juge utile de mentionner : .....
.....
.....
.....
.....
.....
.....

ANNEXES

A.1 NOMENCLATURE DES SYMBOLES ET UNITÉS

Dans les rapports d'essais et autres publications, on utilisera les symboles suivants :

		Unités
A	Superficie du capteur solaire	m^2
A_a	Superficie d'entrée du capteur solaire	m^2
C_p	Capacité thermique massique du fluide caloporteur	J/(kg.k)
E_{ng}	Composante normale de l'éclairement énergétique solaire global tombant sur le plan du capteur	kW/m^2
E_{nt}	Composante normale de l'éclairement énergétique total tombant sur le plan du capteur	kW/m^2
m	Débit massique du fluide caloporteur	kg/s
ΔP	Perte de charge dans le capteur	Pa
Q	Puissance thermique utile du capteur	kW
T_a	Température de l'air ambiant	
T_e	Température d'entrée du fluide caloporteur	
T_s	Température de sortie du fluide caloporteur	°C
T_q	Température de sortie du fluide caloporteur, le capteur ayant atteint un régime d'équilibre	
T_m	Température moyenne de l'absorbeur du capteur	
K	Coefficient de transmission thermique global du capteur	$W/m^2/°C$
α	Coefficient d'absorption des radiations solaires pour l'absorbeur du capteur	
η	Rendement hors tout du capteur $= \frac{Q}{E_{ng} \cdot A}$	
$\frac{\Delta E_{ng}}{\Delta t}$	Variation de la composante normale de l'éclairement énergétique.	

A.2 DÉFINITIONS

A.2.1 Air ambiant

L'air ambiant est l'air extérieur au voisinage du capteur solaire à essayer.

A.2.2 Absorbeur

L'absorbeur est la partie du capteur solaire qui absorbe le rayonnement solaire incident et par laquelle l'énergie est transmise au fluide caloporteur.

A.2.3 Concentrateur

Le concentrateur est la partie du capteur solaire à concentration qui dirige le rayonnement solaire sur l'absorbeur.

A.2.4 Couverture

La couverture est formée d'une ou plusieurs feuilles transparentes montées en avant de la surface absorbante d'un capteur solaire afin de réduire les pertes thermiques de la surface absorbante vers le milieu ambiant, et en vue de protéger des intempéries la dite surface.

A.2.5 Fluide caloporteur

Le fluide caloporteur traverse le capteur solaire et emporte l'énergie thermique utile.

A.2.6 Pyranomètre

Le pyranomètre est un instrument utilisé par les services météorologiques pour mesurer l'éclairement énergétique du rayonnement solaire global sur une surface horizontale.

Dans la présente norme le pyranomètre est utilisé parallèlement au plan d'ouverture du capteur.

On entend par rayonnement solaire global le rayonnement dont le spectre est compris approximativement entre les longueurs d'onde 0,25 μm et 3 μm.

A.2.7 Pyrradiomètre

Le pyrradiomètre est une instrument utilisé pour mesurer l'éclairement énergétique du rayonnement total.

On entend par rayonnement total le rayonnement dont le spectre est compris approximativement entre les longueurs d'onde 0,25 μm et 50 μm.

A.2.8 Superficie du capteur

La superficie du capteur est l'aire de son ombre au soleil sur un plan parallèle au plan d'ouverture, quand le plan d'ouverture du capteur est normal aux rayons du soleil.

A.2.9 Superficie d'entrée

La superficie d'entrée est l'aire de la section droite du rayonnement direct normal pouvant atteindre directement ou par réflexion le volume contenant l'absorbeur.

A.3 CLASSIFICATION DES PYRANOMÈTRES D'APRÈS L'ORGANISATION MÉTÉOROLOGIQUE MONDIALE

	Sensibilité mW/cm²	Stabilité %	Température %	Sélectivité %	Linéarité %	Ouverture	Constante de temps (max)	Réponse cosinus %	Réponse azimut %
Pyranomètre de 1ère classe	± 0,1	± 1	± 1	± 1	± 1	—	25 s	± 3	± 3
Pyranomètre de 2ème classe	± 0,5	± 2	± 2	± 2	± 2	—	1 min	± 5-7	± 5-7
Pyranomètre de 3ème classe	± 1,0	± 5	± 5	± 5	± 3	—	4 min	± 10	± 10